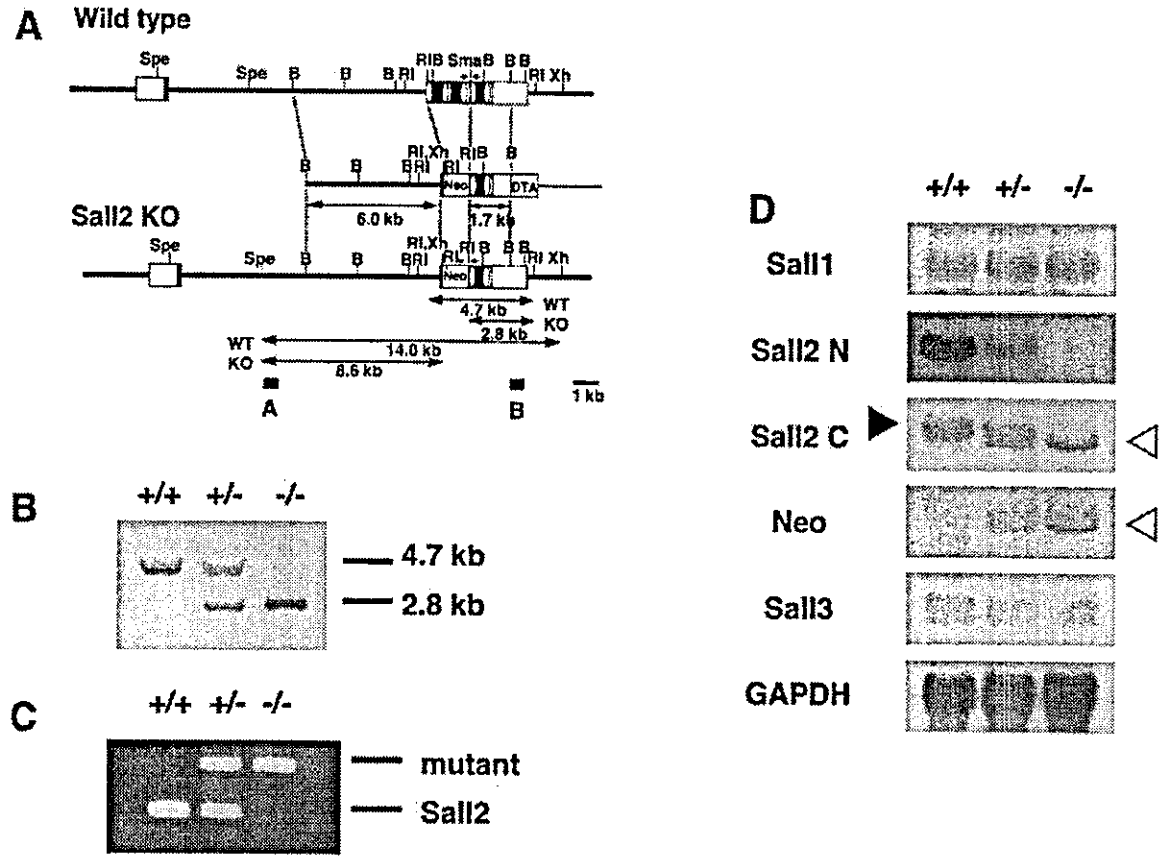

FIG. 1. Generation of *Sall2*-deficient mice. (A) Targeting strategy of *Sall12* locus. Positions of the zinc finger motifs are indicated by ovals. Restriction sites: B, *Bam*HI; RI, *Eco*RI; Spe, *Spe*I; Sma, *Sma*I; Xh, *Xho*I. (B) Southern blot analysis of wild-type (+/+), heterozygous (+/−), and homozygous (−/−) *Sall2*-deficient mice. Tail DNA was digested with *Eco*RI and hybridized with probe B. (C) Genomic PCR of wild-type (+/+), heterozygous (+/−), and homozygous (−/−) *Sall2*-deficient mice. The 388-bp band was amplified from the mutant allele, and the 188-bp band was amplified from the wild-type *Sall2* genome. The positions of the PCR primers are indicated by arrows in panel A. (D) Northern blotting analysis of *Sall* genes in *Sall2*-deficient embryos at 13.5 dpc. Note that N-terminal *Sall2* probe gave no signal in *Sall2*-deficient mice. In the case of the C-terminal *Sall2* probe, the *Sall2* band was absent in *Sall2*-deficient mice (solid arrowhead), but a shorter band appeared that also hybridized with Neo^r probe (open arrowheads).

Histological examination and in situ hybridization. Samples were fixed in 10% formalin and processed for paraffin-embedded sections (6-μm thick), followed by double staining with hematoxylin and eosin.

In situ hybridization was done with digoxigenin-labeled antisense riboprobes as described previously (14). A 1-kb fragment of *Sall2* cDNA corresponding C-terminal three zinc fingers was amplified by using PCR, subcloned into pCRII (Invitrogen), and sequenced. Antisense transcript was generated with SP6 polymerase. Other probes were as described previously (14). None of the sense probes yielded signals.

Peripheral blood count and renal parameter measurement. Cardiac puncture was done in 12-week-old mice, and samples were processed with Celltac α (Nihon Koden, Japan) for peripheral blood counts.

Next, 10- to 14-month-old mice were used to measure blood urea nitrogen and creatinine in serum with an automatic analyzer 7150 (Hitachi, Tokyo, Japan). Urinary protein was measured by using Pretest (Wako, Tokyo, Japan) containing tetrabromophenol blue.

RESULTS AND DISCUSSION

Generation of *Sall2*-deficient mice. To examine developmental functions, we inactivated *Sall2* in the mouse by using embryonic stem cells (Fig. 1A). The *Sall2* gene consists of two exons, the intron being ca. 12 kb. All eight zinc finger domains are located in exon 2. We generated a targeting construct, which deleted the N-terminal five zinc fingers. Chimeras from two independent homologous recombinants transmitted the mutations through the germ line. Mice were genotyped by using Southern blots and genomic PCR (Fig. 1B and C). Northern blots confirmed that full-length *Sall2* transcript was indeed absent in *Sall2*-deficient mice, with either the N-terminal region or the C-terminal region of *Sall2* as a probe (Fig. 1D). Probing with the C-terminal region of *Sall2*, however, showed a slightly shorter transcript in heterozygous and homozygous mice and was expressed more abundantly in the latter. This transcript was also evident with a Neo^r probe, indicating that it may be a transcript that read through the poly(A) addition signal of Neo^r and fused to C-terminal *Sall2* (Fig. 1D). We isolated this cDNA from *Sall2*-deficient mice and found that this was indeed the case. There were several stop codons in the junction and the *Sall2* region was out of frame (data not shown). There were no other irregular transcripts indicative of aberrant *Sall2* molecules. Therefore, it is unlikely that the functional C-terminal protein of Sall2 was expressed in the mutant mice. Expression of *Sall1* and *Sall3*

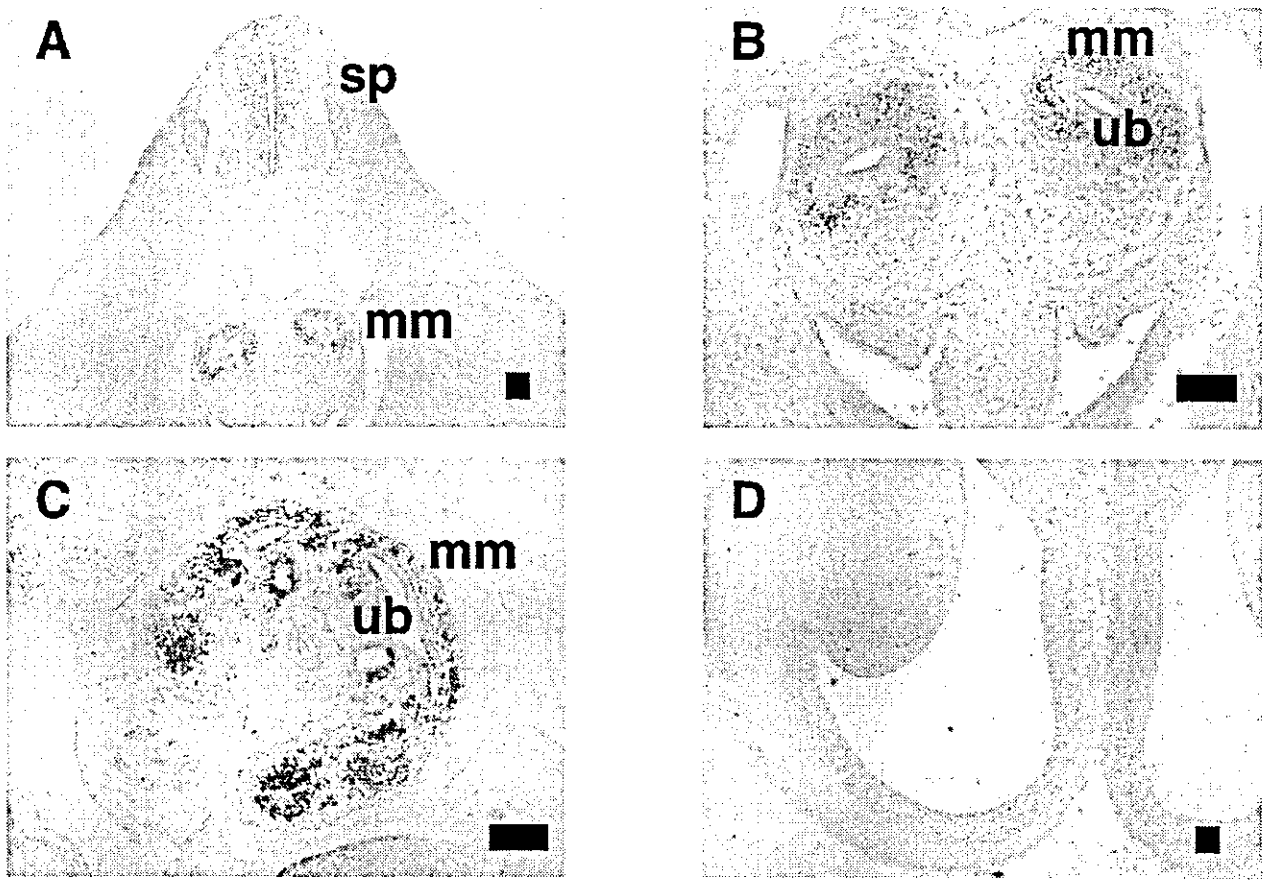

FIG. 2. Expression of *Sall2* in developing embryos. (A) Metanephros and spinal cord at 11.5 dpc (sp, spinal cord; mm, metanephric mesenchyme); (B) metanephros at 11.5 dpc (ub, ureteric bud; mm, metanephric mesenchyme); (C) metanephros at 13.5 dpc; (D) brain at 14.5 dpc. Scale bar, 100 μm.

was not altered in the absence of *Sall2*, as determined by using Northern blots (Fig. 1D).

Expression patterns of Sall2. Transverse sections obtained 11.5 dpc showed *Sall2* expression in the metanephric mesenchyme surrounding the ureteric bud and subventricular region of the spinal cord (Fig. 2A,B). At 13.5 dpc, *Sall2* expression was observed in the mesenchyme around the ureteric buds in the cortical regions of the developing kidney (Fig. 2C). *Sall2* was also expressed in the subventricular zone of the brain at 14.5 dpc (Fig. 2D). This expression pattern partly overlaps that of mouse *Sall1* (3, 14, 16).

Normal phenotypes in Sall2-deficient mice. No obvious phenotype was observed in the heterozygous mutants. When heterozyotes were intercrossed, the homozygous mice were of Mendelian frequency (Table 1), they had a normal appearance, and both male and female homozygotes were fertile. We found no abnormalities despite extensive anatomical examinations. Figure 3A to F show an almost-normal histology of the *Sall2* mutant kidney, heart, and ears at 13.5 dpc. The hematological parameters of peripheral blood samples were also normal (Table 2).

The expression patterns of well-characterized molecular markers of either metanephric mesenchyme or ureteric bud-derived cells were also examined.

Sall1 is expressed in the metanephric mesenchyme, and the expression of *Sall1* was not altered in the absence of *Sall2*, findings consistent with the data in Fig. 1D (Fig. 4A and B).

Pax2-deficient mice do not develop mesonephric tubules and lack ureteric buds (21). In metanephros at 13.5 dpc, *Pax2* is expressed both in the ureteric bud and in the condensed mesenchyme surrounding the ureteric bud (Fig. 4C). In *Sall2* mutant mice, the expression of *Pax2* was unaltered in both these locations (Fig. 4D).

Wnt4 is required for epithelialization of the induced mesenchyme but not for the initial induction by the ureter (20). *Wnt4* is expressed in mesenchymal cells on the sides of the ureteric bud and correlates to the site where the first pretubular aggre-

TABLE 1. Genotype analysis of mice from *Sall2* heterozygous intercrosses[a]

Mouse	*n*	% of total
+/+	26	27.7
+/−	46	48.9
−/−	22	23.4

[a] DNA was extracted from the tails of 3-week-old mice and analyzed by using PCR as for Fig. 1C.

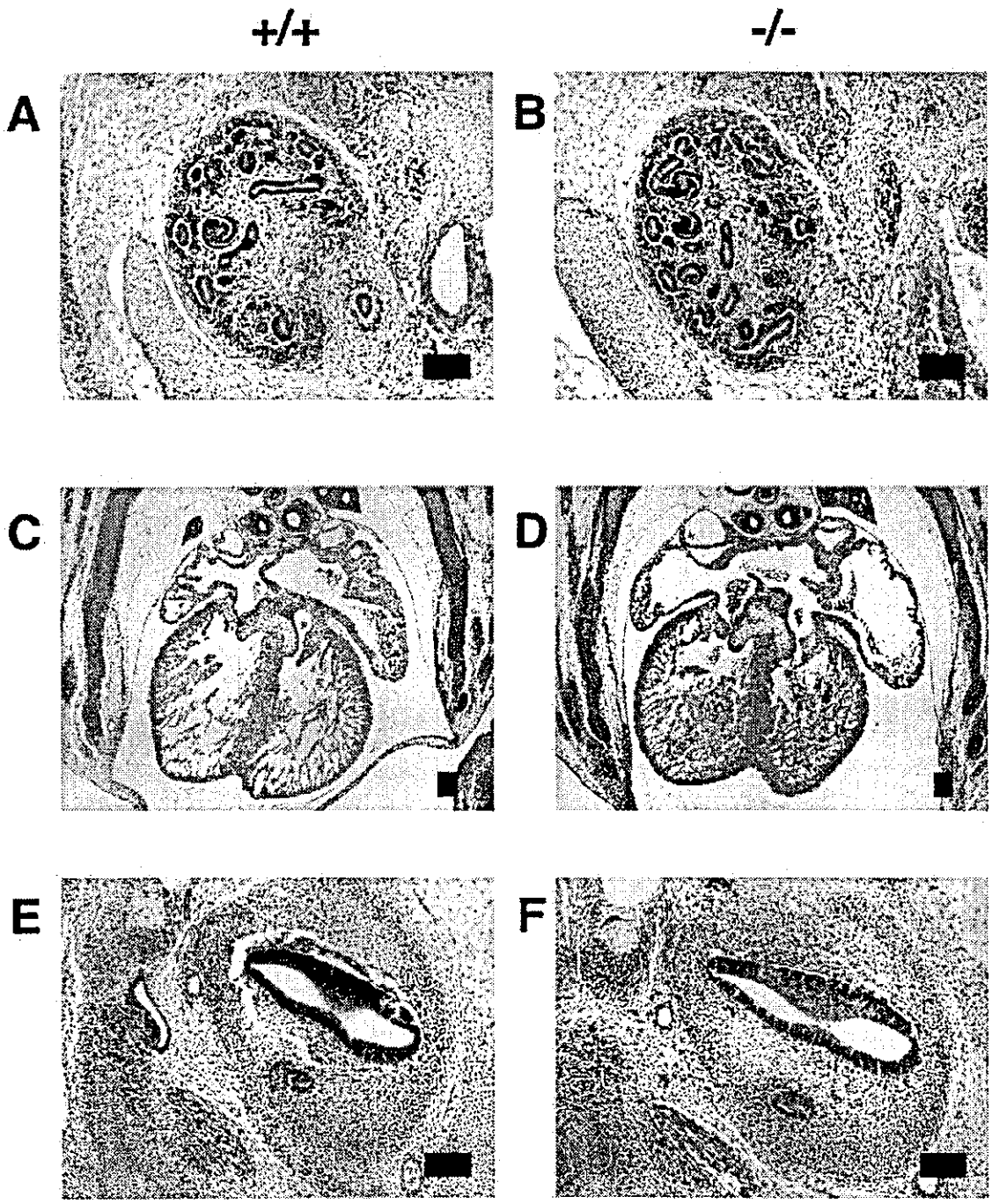

FIG. 3. Histology in *Sall2*-deficient mice at 13.5 dpc. (A and B) Kidneys in wild-type (A) and *Sall2*-deficient mice (B); (C and D) hearts in wild-type (C) and *Sall2*-deficient mice (D); (E and F) inner ears in wild-type (E) and *Sall2*-deficient mice (F). Scale bars, 100 μm.

gates form (Fig. 4E). *Sall2*-deficient mice showed unaltered *Wnt4* expression (Fig. 4F).

Mice deficient in the tyrosine-kinase type receptor, *Ret*, show a failure of ureteric bud invasion and subsequent failure of mesenchymal differentiation (12, 17–19). *Ret* was expressed in the ureteric bud in the wild type, and its expression in *Sall2* mutant mice was unaltered (Fig. 4G and H). These results

TABLE 2. Peripheral blood counts of *Sall2*-deficient mice

Mouse (*n*)	Mean amt (SD)				
	Leukocytes (10^3/μl)	Erythrocytes (10^6/μl)	Hemoglobin (g/dl)	Hematocrit (%)	Platelets (10^3/μl)
+/+ (9)	8.0 (2.4)	8.7 (2.9)	16.1 (1.6)	52.9 (6.8)	920 (248)
+/− (6)	10.6 (5.5)	9.5 (1.4)	16.6 (1.5)	51.7 (7.0)	821 (86)
−/− (8)	9.9 (3.8)	10.1 (0.6)	17.1 (0.8)	54.9 (2.7)	819 (117)

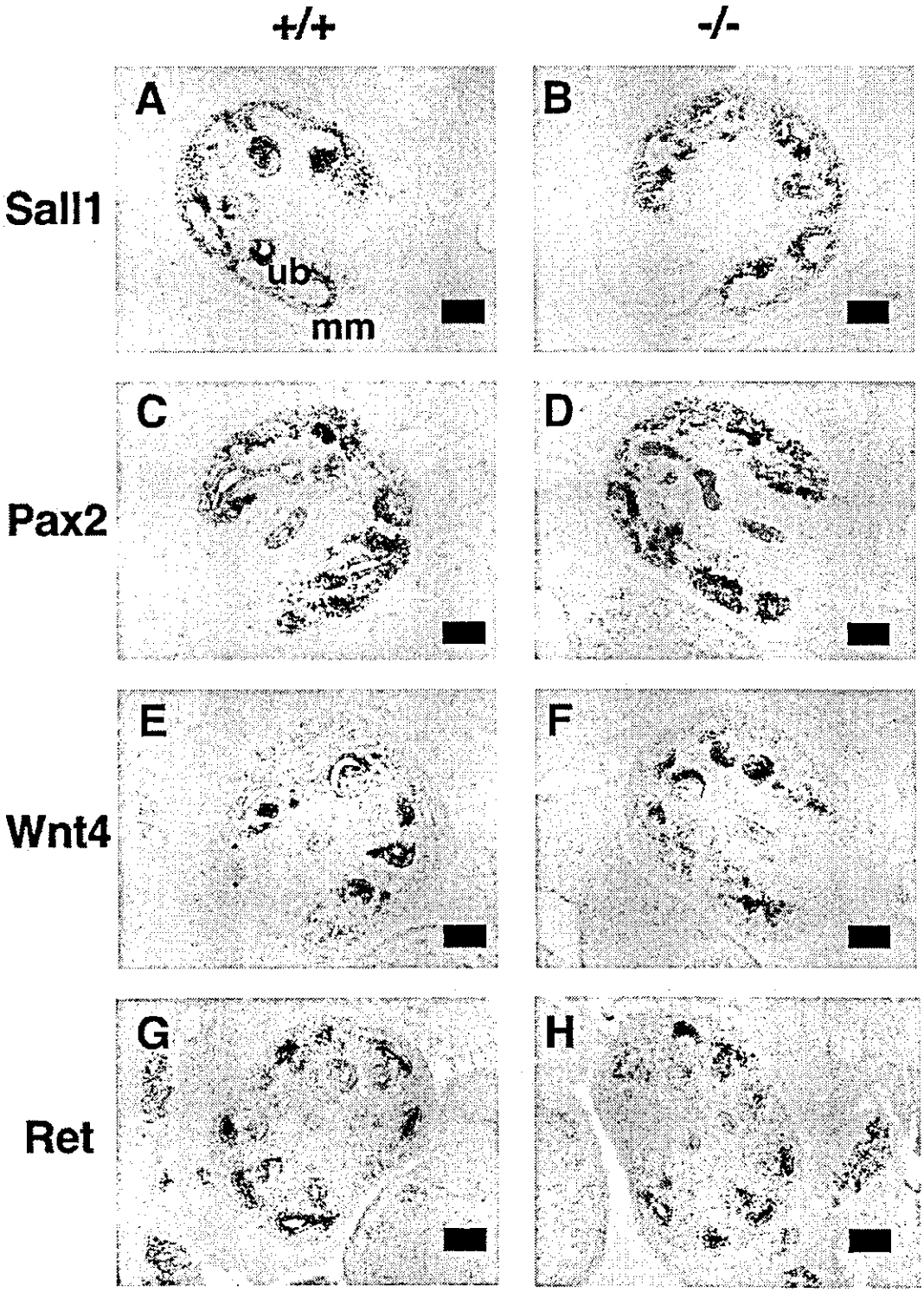

FIG. 4. In situ hybridization of molecular markers in 13.5-dpc metanephros of wild-type (left panels [A, C, E, and G]) and *Sall2*-deficient mice (right columns [B, D, F, and H]). Scale bars, 100 μm. (A and B) *Sall1*; (C and D) *Pax2*; (E and F) *Wnt4*; (G and H) *Ret*.

TABLE 3. Genotype analysis of mice from *Sall1*$^{+/-}$ *Sall2*$^{-/-}$ intercrosses[a]

Sall1	*Sall2*	*n*	% of total
+/+	−/−	12	23.1
+/−	−/−	28	53.8
−/−	−/−	12	23.1

[a] DNA was extracted from the tails of newborn mice and analyzed by using PCR.

indicate that markers of metanephric mesenchyme and ureteric bud were not affected in the absence of *Sall2* and that *Sall2* is not required for normal kidney development.

There was no limb deformity, anorectal anomaly, or ear anomaly, all of which are characteristic of Townes-Brocks syndrome, which is caused by *SALL1* mutation. We suggest that

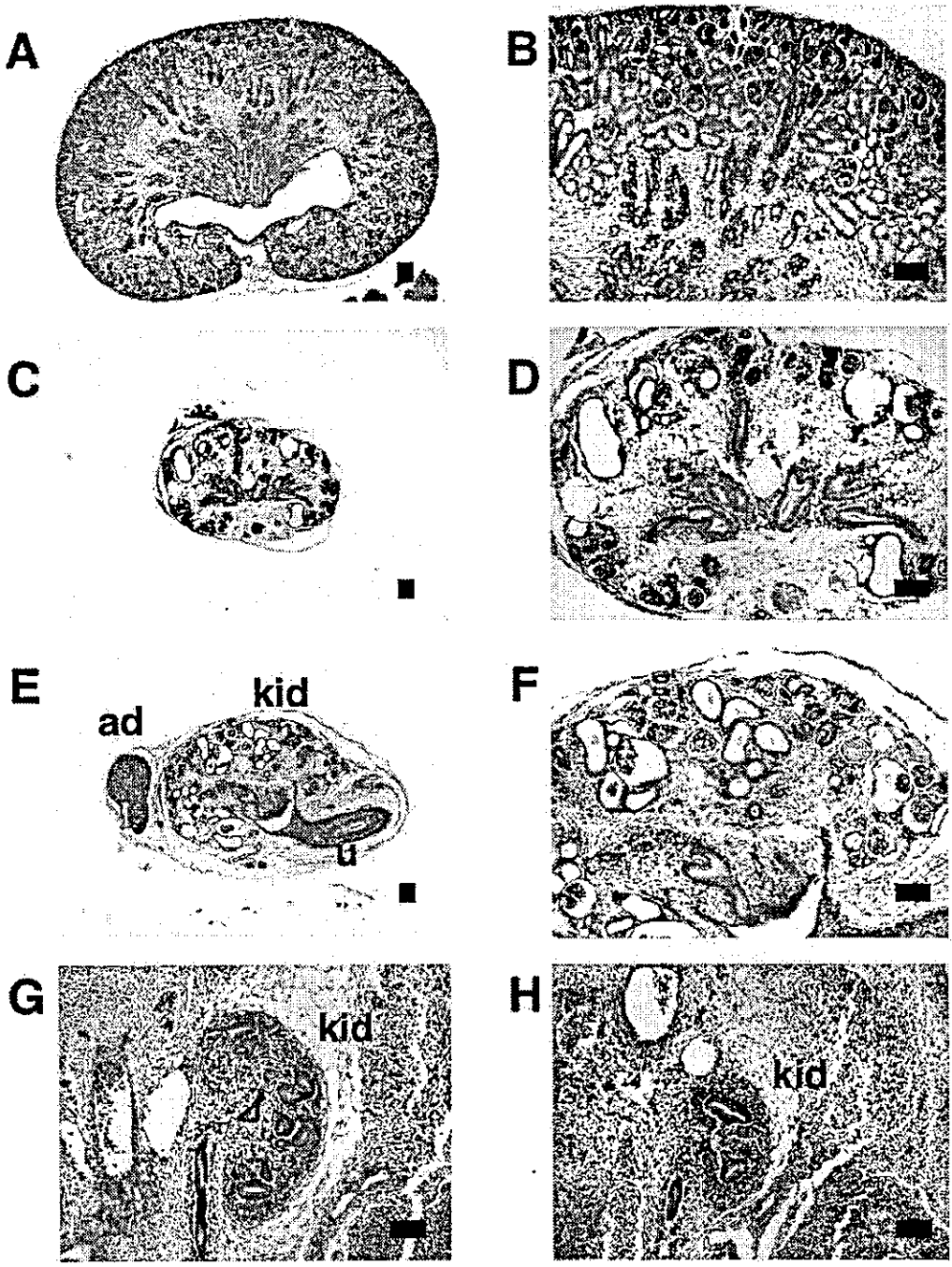

FIG. 5. Kidney development in *Sall1/2* double deficient mice. (A and B) Kidney of wild-type newborn. (C and D) Kidney of *Sall1/2* double deficient mice. The kidney is small and contains multiple cysts. (E and F) Kidney of *Sall1*-deficient mice, which shows a similar histology to *Sall1/2* doubly deficient mice. (G) Metanephros in wild-type mice at 12.5 dpc. Branching is evident. (H) Metanephros in *Sall1/2* doubly deficient mice at 12.5 dpc. Kidney size and ureteric branching are reduced. kid, kidney; ad, adrenal gland; u, ureter. Scale bars, 100 μm.

TABLE 4. Renal function in adult animals[a]

Sall1	*Sall2*	*n*	Mean level (SD)	
			BUN[b] (mg/dl)	Creatinine (mg/dl)
+/+	+/+	5	27.3 (2.4)	0.30 (0.03)
+/−	+/−	8	28.7 (3.4)	0.29 (0.04)
+/+	−/−	8	24.5 (4.3)	0.31 (0.04)
+/−	−/−	7	24.0 (4.1)	0.31 (0.03)

[a] Ten- to fourteen-month-old mice were used.
[b] BUN, blood urea nitrogen.

Sall2 is not essential for development and that *Sall2* absence may be compensated for by other *Sall* genes, the expression of which overlaps with that of *Sall2*.

Human *SALL2* is located on chromosome 14q12, possibly overlapping a region of loss of heterozygosity in ovarian cancers (1). In addition, mouse *Sall2* binds to polyomavirus large T antigen and was proposed to be a potential tumor suppressor (11). *Sall2* mutant mice, however, did not show spontaneous tumor formation for more than 1 year after birth. Tumor formation upon virus inoculation will be required to test the hypothesis that *Sall2* is a tumor suppressor.

Kidney defects in mice lacking both *Sall1* and *Sall2*. Mouse *Sall1* is essential for the initial step for metanephros formation: ureteric bud attraction. Hence, kidney agenesis or severe dysgenesis was present in *Sall1*-deficient mice. Other organs, however, were not affected, although heterozygous mutations of human *SALL1* lead to Townes-Brocks syndrome, with features of dysplastic ears, preaxial polydactyly, imperforate anus, and heart anomalies in addition to kidney anomalies. The relative importance of *SALL1* over *SALL2* and *-3* may be higher in humans than in mice, and *Sall1* deficiency may be compensated for by *Sall2* and *-3* in mice.

To address this question, we crossed *Sall1* and *Sall2* mutants and generated mice lacking both genes. Some pups from a double heterozygous cross were dead perinatally and had kidney abnormalities; most were *Sall1* single mutants, but we did find some double homozygotes. To further confirm the phenotypes, we set up pairs of $Sall1^{+/-}$ $Sall2^{-/-}$ mice and found that double mutants were born at a Mendelian frequency (Table 3). All of the double mutants, as well as the *Sall1* mutants, were dead perinatally, and they all had kidney abnormalities. Of 12 double mutants (25.0%), 3 had no kidneys or ureters bilaterally. Four mice (33.3%) had unilateral kidney agenesis and hypoplasia on the other side. Five mice (41.7%) had two small remnant kidneys. Histological examination of all of the residual kidneys in the double mutant newborn showed size reduction and multiple cysts, which are comparable to the *Sall1* mutants (Fig. 5A to F). At 12.5 dpc, size reduction and impaired ureteric branching were observed in *Sall1*/2-null mutants, which is also comparable to findings in the *Sall1* mutants (Fig. 5G and H and data not shown). Thus, the severity of the kidney impairment of the double mutants was comparable to that of *Sall1* single mutants reported earlier (14), indicating that *Sall2* absence does not exacerbate the kidney defects caused by *Sall1* mutation.

To address the role of *Sall* genes in maintaining renal function in adults, several parameters were examined in aged $Sall1^{+/-}$ $Sall2^{-/-}$ mutants, as well as in $Sall1^{+/-}$ $Sall2^{+/-}$ mutants, *Sall2* single mutants, and wild-type control (Table 4). Blood urea nitrogen and creatinine levels in serum were not significantly different among the four groups. Urinary protein was undetectable in all animals tested. Although these parameters are not sensitive enough for detecting minor renal malfunction, the data do suggest that the absence of *Sall2* or reducing *Sall1* dosage upon *Sall2* mutant background does not lead to overt kidney diseases in adult mice.

Furthermore, the double mutants showed no phenotypes of Townes-Brocks syndrome, such as dysplastic ears, preaxial polydactyly, and imperforate anus. These data suggest that the discrepancy of the mutant phenotypes of human *SALL1* and mouse *Sall1* cannot be explained by compensation by *Sall2* in mice. Generation of mice lacking all of the *Sall* genes will be necessary in order to address the developmental roles of *Sall* genes.

ACKNOWLEDGMENT

The Division of Stem Cell Regulation is supported by Amgen Limited.

REFERENCES

1. **Bandera, C. A., H. Takahashi, K. Behbakht, P. C. Liu, V. A. LiVolsi, I. Benjamin, M. A. Morgan, S. A. King, S. C. Rubin, and J. Boyd.** 1997. Deletion mapping of two potential chromosome 14 tumor suppressor gene loci in ovarian carcinoma. Cancer Res. 57:513–515.
2. **Buck, A., L. Archangelo, C. Dixkens, and J. Kohlhase.** 2000. Molecular cloning, chromosomal localization, and expression of the murine *SALL1* ortholog *Sall1*. Cytogenet. Cell Genet. 89:150–153.
3. **Buck, A., A. Kispert, and J. Kohlhase.** 2001. Embryonic expression of the murine homologue of SALL1, the gene mutated in Townes-Brocks syndrome. Mech. Dev. 104:143–146.
4. **de Celis, J. F., R. Barrio, and F. C. Kafatos.** 1996. A gene complex acting downstream of *dpp* in *Drosophila* wing morphogenesis. Nature 381:421–424.
5. **Jurgens, G.** 1988. Head and tail development of the *Drosophila* embryos involves *spalt*, a novel homeotic gene. EMBO J. 7:189–196.
6. **Kohlhase, J., M. Altmann, L. Archangelo, C. Dixkens, and W. Engel.** 2000. Genomic cloning, chromosomal mapping, and expression analysis of *msal-2*. Mamm. Genome 11:64–68.
7. **Kohlhase, J., S. Hausmann, G. Stojmenovic, C. Dixkens, K. Bink, W. Schulz-Schaeffer, M. Altmann, and W. Engel.** 1999. *SALL3*, a new member of the human *spalt*-like gene family, maps to 18q23. Genomics 62:216–222.
8. **Kohlhase, J., R. Schuh, G. Dowe, R. P. Kuhnlein, H. Jackle, B. Schroeder, W. Schulz-Schaeffer, H. A. Kretzschmar, A. Kohler, U. Muller, M. Raab-Vetter, E. Burkhardt, W. Engel, and R. Stick.** 1996. Isolation, characterization, and organ-specific expression of two novel human zinc finger genes related to the *Drosophila* gene *spalt*. Genomics 38:291–298.
9. **Kohlhase, J., A. Wischermann, H. Reichenbach, U. Froster, and W. Engel.** 1998. Mutations in the *SALL1* putative transcription factor gene cause Townes-Brocks syndrome. Nat. Genet. 18:81–83.
10. **Kuhnlein, R. P., G. Frommer, M. Friedrich, M. Gonzalez-Gaitan, A. Weber, J. F. Wagner-Bernholz, W. J. Gehring, H. Jackle, and R. Schuh.** 1994. *spalt* encodes an evolutionarily conserved zinc finger protein of novel structure which provides homeotic gene function in the head and tail region of the *Drosophila* embryo. EMBO J. 13:168–179.
11. **Li, D., K. Dower, Y. Ma, Y. Tian, and L. T. Benjamin.** 2001. A tumor host range selection procedure identifies $p150^{Sal2}$ as a target of polyoma virus large T antigen. Proc. Natl. Acad. Sci. USA 98:14619–14624.
12. **Moore, M. W., R. D. Klein, I. Farinas, H. Sauer, M. Armanini, H. Phillips, L. F. Reichardt, A. M. Ryan, K. Carver-Moore, and A. Rosenthal.** 1996. Renal and neuronal abnormalities in mice lacking GDNF. Nature 382:76–79.
13. **Nellen, D., R. Burke, G. Struhl, and K. Basler.** 1996. Direct and long-range action of a DPP morphogen gradient. Cell 85:357–368.
14. **Nishinakamura, R., Y. Matsumoto, K. Nakao, K. Nakamura, A. Sato, G. N. Copeland, J. D. Gilbert, A. N. Jenkins, S. Scully, L. D. Lacey, M. Katsuki, M. Asashima, and T. Yokota.** 2001. Murine homolog of *Sall1* is essential for ureteric bud invasion in kidney development. Development 128:3105–3115.
15. **Ott, T., K. H. Kaestner, A. P. Monaghan, and G. Schutz.** 1996. The mouse homolog of the region specific homeotic gene *spalt* of *Drosophila* is expressed in the developing nervous system and in mesoderm-derived structures. Mech. Dev. 56:117–128.
16. **Ott, T., M. Parrish, K. Bond, A. Schwaeger-Nickolenko, and A. P. Monaghan.** 2001. A new member of the spalt like zinc finger protein family, Msal3, is expressed in the CNS and sites of epithelial/mesenchymal interaction. Mech. Dev. 101:203–207.

17. **Pichel, J. G., L. Shen, H. Z. Sheng, A. C. Granholm, J. Drago, A. Grinberg, E. J. Lee, S. P. Huang, M. Saarma, B. J. Hoffer, H. Sariola, and H. Westphal.** 1996. Defects in enteric innervation and kidney development in mice lacking GDNF. Nature 382:73–76.
18. **Sanchez, M. P., I. Silos-Santiago, J. Frisen, B. He, S. A. Lira, and M. Barbacid.** 1996. Renal agenesis and the absence of enteric neurons in mice lacking GDNF. Nature 382:70–73.
19. **Schuchardt, A., V. D'Agati, L. Larsson-Blomberg, F. Costantini, and V. Pachnis.** 1994. Defects in the kidney and enteric nervous system of mice lacking the tyrosine kinase receptor Ret. Nature 367:380–383.
20. **Stark, K., S. Vainio, G. Vassileva, and A. P. McMahon.** 1994. Epithelial transformation of metanephric mesenchyme in the developing kidney regulated by Wnt-4. Nature 372:679–683.
21. **Torres, M., E. Gomez-Pardo, G. R. Dressler, and P. Gruss.** 1995. Pax-2 controls multiple steps of urogenital development. Development 121:4057–4065.

Original Article

Transmural Pressure Control of Prorenin Processing and Secretion in Diabetic Rat Juxtaglomerular Cells

Nobuhisa HIROTA, Atsuhiro ICHIHARA, Yukako KOURA, Yuko TADA, Matsuhiko HAYASHI, and Takao SARUTA

In diabetic patients, the elevation of plasma prorenin levels or arterial pressure is correlated with the severity of diabetic nephropathy. This study was designed to assess the effects of transmural pressure on prorenin regulation in juxtaglomerular (JG) cells from diabetes rats. The JG cells, harvested from rats intraperitoneally injected with streptozotocin 7 (early-diabetic) or 28 (late-diabetic) days previously, were exposed to atmospheric pressure (AP) and AP+40 mmHg for 12 h, and the renin secretion rate (RSR), prorenin secretion rate (PRSR), active renin content (ARC), prorenin content (PRC), and total renin content (TRC) were determined. Exposure of control JG cells to AP+40-mmHg significantly decreased RSR, PRSR, and ARC and significantly increased PRC without affecting TRC, suggesting the occurrence of pressure-mediated inhibition of prorenin processing and secretion. Exposure of early-diabetic and late-diabetic cells to AP+40-mmHg significantly decreased ARC and significantly increased PRC without affecting RSR, PRSR, or TRC. The changes in ARC and PRC were similar in the control and early-diabetic cells, but greater changes were observed in late-diabetic cells. However, when streptozotocin-treated rats were continuously treated with insulin (9 U/kg/day), the transmural pressure control of prorenin in JG cells was similar to that observed in the JG cells from control rats. In late-diabetic cells, treatment with a phospholipase C inhibitor did not alter the pressure control of ARC or PRC; however, treatment with a phospholipase D inhibitor did inhibit the changes in ARC and PRC with transmural pressure. Thus, pressure-mediated inhibition of prorenin secretion from JG cells has already been impaired in early diabetes. Pressure-induced inhibition of prorenin processing in JG cells *via* phospholipase D-dependent pathways is enhanced in late diabetes.
(*Hypertens Res* 2003; 26: 493–501)

***Key Words*: mechanoreceptors, renin, kidney, streptozotocin, phospholipase**

Introduction

The most striking abnormality of the renin-angiotensin system components in the blood of diabetics is an increase in prorenin levels (*1*), although the renin-angiotensin system makes an important contribution to the development and progression of diabetic nephropathy (2). The elevation of the plasma prorenin level precedes the onset of microalbuminuria (*3–5*) and is correlated with the severity of diabetic microvascular complications (*6, 7*). These lines of evidence imply an essential role of prorenin in the development and progression of diabetic nephropathy. In addition, the United Kingdom Prospective Diabetes Study demonstrated that lowering blood pressure itself reduces the risk of macrovascular and microvascular complications in type 2 diabetic patients independent of the class of antihypertensive drugs used to treat them (*8–10*), suggesting that arterial pressure also con-

From the Department of Internal Medicine, Keio University School of Medicine, Tokyo, Japan.
This work was supported in part by a Grant-in-Aid for Scientific Research from the Ministry of Education, Culture, Sports, Science and Technology, Japan (14571073) and a grant from the Magnetic Health Science Foundation, Tokyo, Japan.
Address for Reprints: Atsuhiro Ichihara, M.D., Internal Medicine, Keio University School of Medicine, 35 Shinanomachi, Shinjuku-ku, Tokyo 160–8582, Japan. E-mail: atzichi@sc.itc.keio.ac.jp
Received November 18, 2002; Accepted in revised form January 23, 2003.

tributes to the progression of diabetic nephropathy and coronary vascular diseases (*11*). We recently showed that a chronic transmural pressure load decreases active renin concentration without affecting total renin concentration in rat juxtaglomerular (JG) cells, suggesting that transmural pressure inhibits conversion of prorenin to active renin and as a result increases intracellular prorenin levels in JG cells (*12*). However, the effects of transmural pressure on prorenin secretion and intracellular prorenin content in JG cells harvested from diabetic rats remain undetermined.

The present study was designed to identify the effects of a chronic transmural pressure load on prorenin processing and secretion in diabetic JG cells. Diabetic JG cells were harvested from rats intraperitoneally injected with streptozotocin 7 and 28 days previously to determine whether any differences in pressure control of prorenin existed between the early and late stages of diabetes mellitus. Experiments were also performed in diabetes rat JG cells exposed to a buffer containing a phospholipase C (PLC) inhibitor or a phospholipase D (PLD) inhibitor to determine the contribution of phospholipase-dependent pathways to pressure control of prorenin regulation in diabetes.

Methods

Animal Preparation

Male Sprague-Dawley rats weighing 100 to 150 g (Charles River Japan, Yokohama, Japan) were housed in wire cages and maintained in a temperature-controlled room with a 12-h light/12-h dark cycle. Rats had free access to water and standard laboratory chow containing 110 μmol/g of sodium (Oriental Yeast, Tokyo, Japan). Animals were intraperitoneally injected with 65 mg/kg of streptozotocin (Wako, Osaka, Japan) or 10 mmol/l citrate buffer without streptozotocin, as a control. The onset and maintenance of diabetes were confirmed by blood glucose levels greater than 300 mg/dl at 7 days and 28 days, respectively, after the injection. All experiments were performed in accordance with the guidelines and practices established by the Keio University Animal Care and Use Committee. For one experiment, JG cells were harvested from the kidneys of ten rats.

Primary Culture of Rat JG Cells

JG cells were isolated from the kidneys of the rats 7 days and 28 days after the injection of streptozotocin or control buffer, as previously described (*12–15*), and used as early- and late-stage diabetic JG cells, respectively. The JG cells were suspended at a density of 10^6 cells/ml in culture medium consisting of RPMI 1640 with 25 mmol/l HEPES, 0.3 g/l L-glutamine, 100 μg/ml streptomycin, 100 U/ml penicillin, 0.66 U/l insulin, and 10% fetal bovine serum (FBS). Cell number was determined with a Coulter counter (Coulter, Miami, USA). The suspended cells were distributed in 1 ml aliquots into individual wells of 8-well chamber slides containing 1 ml of culture medium, and then incubated at 37 °C. JG cells were allowed to rest for 48 h before beginning the experiments. Immunofluorescence staining for renin at 60 h after isolation confirmed that 92±2% of the cells (n=6 primary cultures) were renin-positive.

Pressure-Loading of JG Cells

JG cells were exposed to pressure with a minimal contribution of shear stress or stretch, as reported previously (*12*). The 8-well chamber slides were placed in a sanitary pressure vessel (model: DV-5-ST; Advantec Toyo, Tokyo, Japan) pre-warmed to 37 °C. The pressure vessel was then sealed tightly, and connected to tubing attached to a three-way rotary valve, a sphygmomanometer, and a pressure valve. Compressed helium was pumped in to raise the internal pressure, and the sanitary pressure vessel was placed in an incubator with the internal temperature maintained at a constant 37 °C. The pressure level was monitored with a sphygmomanometer during the experiments. The partial pressure of oxygen and the pH of the medium averaged 155±4 mmHg and 7.4±0.1, respectively, and were kept constant throughout the experiments. In the present study, the JG cells were also subjected to transmural pressures equal to atmospheric pressure (AP) and AP+40 mmHg. To estimate the transmural pressure directly affecting cell membranes of JG cells, a vessel that had a pressure sensor at the bottom and that had been filled with 1 ml buffer was pressurized to 40 mmHg. The actual increase in pressure at the bottom of the vessel averaged 36.6±0.7 mmHg (n=10).

Measurement of Renin Secretion Rate, Prorenin Secretion Rate, Active Renin Content, Prorenin Content, and Total Renin Content of JG Cells

The renin secretion rate (RSR), prorenin secretion rate (PRSR), active renin content (ARC), prorenin (inactive renin) content (PRC), and total (active+inactive) renin content (TRC) were measured in JG cells as described previously (*12, 15*). In brief, after removing the culture medium, the cells were washed twice with pre-warmed phosphate buffered saline (PBS), and each well was filled with 1 ml of Ca^{2+}-containing PBS and placed in the pressure-loading apparatus. Immediately before (0 h) and 12 h after pressure loading, the cell-conditioned buffer was removed and centrifuged. The supernatants were stored at −20 °C until active and total renin activity was assayed to determine RSR and PRSR. After rinsing with PBS, the cells were frozen in liquid nitrogen and stored at −80 °C. For assay of ARC, PRC, and TRC, frozen cells were homogenized in 1 ml of buffer (pH 6.0) containing 2.6 mmol/l ethylenediaminetetraacetate, 1.6 mmol/l dimercaprol, 3.4 mmol/l 8-hydroxyquinoline sulfate, 0.2 mmo/l phenylmethylsulfonyl fluoride, and 5 mmol/l ammonium acetate. The homogenates were centrifuged at

12,000×*g* for 30 min, and the supernatant was removed. To measure the total renin activity in the buffer and the TRC in the JG cells, the samples were incubated at 0°C for 60 min with 100 μl of 4 mg/ml trypsin (Sigma Chemical Co., St Louis, USA) in 500 mmol/l Tris buffer, pH 7.5, containing 5 mmol/l $CaCl_2$, 0.1% NaCl azide, and 1% bovine serum albumin. Soybean trypsin inhibitor (Sigma Chemical Co., 8 mg/ml final concentration) was added to stop the reaction. By so doing, the inactive renin in the samples was converted to active renin, and the renin activity was then determined.

Renin activity was determined as previously described (*14*). Samples were incubated for 1 h at 37°C with plasma from bilaterally nephrectomized male Sprague-Dawley rats as the renin substrate, and renin activity was determined by angiotensin (Ang) I generation from a plasma angiotensinogen substrate. Ang I levels were measured with a radioimmunoassay coated-bead kit from Dinabott Radioisotope Institute (Tokyo, Japan). RSR (%) was calculated as the fractional release of overall active renin (*i.e.*, [buffer renin activity at 12h−buffer renin activity at 0h] / [active renin content in JG cells at 12h+buffer renin activity at 12h−buffer renin activity at 0h]). PRSR (%) was calculated as the fractional release of overall inactive renin (*i.e.*, [buffer inactive renin activity at 12h−buffer inactive renin activity at 0h] / [inactive renin content in JG cells at 12h+buffer inactive renin activity at 12h−buffer inactive renin activity at 0h]). The buffer inactive renin activity and the PRC of JG cells were calculated respectively by subtraction of the buffer active renin activity from the buffer total renin activity of JG cells and by subtraction of the ARC from the TRC of JG cells. JG-cell ARC, PRC, and TRC were expressed as renin activity per million cells in the sample obtained.

Experimental Protocols

Primary JG cell culture wells were divided into two groups, wells exposed to AP for 12 h and wells exposed to AP+40 mmHg for 12 h. Each group consisted of at least 2 wells, and the mean values per primary culture were determined in each group. To assess the effect of a chronic transmural pressure load on prorenin processing and secretion, the RSR, PRSR, ARC, PRC, and TRC values of the AP- and AP+40 mmHg-loaded JG cells were compared. In the first series of experiments, we assessed the transmural pressure control of prorenin processing and secretion in JG cells harvested from the rats 7 days after intraperitoneal injection of streptozotocin or control buffer. In the second series of experiments, transmural pressure control of prorenin processing and secretion was assessed in JG cells harvested from rats 28 days after intraperitoneal injection of streptozotocin or control buffer. In the third series of experiments, to exclude possible non-glycemic effects of streptozotocin on transmural pressure control of prorenin processing and secretion, three osmotic minipumps (model 2004; Alzet, Palo Alto, USA) were implanted into the dorsal neck and peritoneal cavity of each rat. The minipumps continuously delivered regular insulin (9 U/kg/day, Novolin R; Novo Nordisc Pharma, Tokyo, Japan) to streptozotocin-treated rats for a 4-week period. Blood glucose levels were measured twice weekly. JG cells of the insulin-treated diabetes rats were harvested 28 days after injection of streptozotocin, and the pressure load study was performed. In the fourth series of experiments, to examine the contribution of PLC- and PLD-dependent pathways to transmural pressure control of prorenin processing and secretion in diabetes, the JG cells harvested from rats 28 days after intraperitoneal injection of streptozotocin were conditioned in buffer containing the PLC inhibitor 2-nitro-4-carboxyphenyl-*N*,*N*-diphenyl-carbamate (NCDC, 200 μmol/l; Sigma Chemical Co.) or the PLD inhibitor 4-(2-aminoethyl)-benzensulfonyl fluoride (AEBSF, 100 μmol/l; Sigma Chemical Co.) during the pressure load, as previously described (*15*).

Statistical Analysis

Data were analyzed by two-way analysis of variance (ANOVA) followed by multiple comparisons using Scheffé's *F*-test for repeated measures. A value of $p<0.05$ was considered statistically significant. Data are shown as the means ±SEM.

Results

Transmural Pressure Controls of Prorenin in Early-Stage Diabetes

Table 1 shows body weight, systolic blood pressure, urinary protein excretion, and blood glucose levels of control and diabetes rats at the early (7 days) and late (28 days) stages after the injections. Compared to control rats, early-stage diabetes rats had lower body weights, higher levels of blood glucose, and similar levels of systolic blood pressure and urinary protein excretion. Figure 1 shows the effects of 12-h exposure to transmural pressure on RSR and PRSR in JG cells harvested from the rats intraperitoneally injected with control buffer or streptozotocin 7 days previously. In the control rat JG cells, exposure to AP+40 mmHg-transmural pressure significantly decreased RSR from 61.8±1.3% to 24.4±4.4% and PRSR from 13.6±1.5% to 4.5±1.5%. In the JG cells from rats with early-stage streptozotocin-induced diabetes, RSR under AP averaged 42.5±3.5% and was significantly less than the RSR in control rat JG cells. PRSR under AP averaged 28.3±4.0% and was significantly greater than the PRSR in control rat JG cells. Neither RSR nor PRSR was altered by exposure to AP+40 mmHg-transmural pressure (45.9±3.7% and 25.5±3.1%, respectively). Thus, the pressure-induced decreases in RSR and PRSR were abolished in the early stage of diabetes mellitus.

Figure 2 demonstrates that exposure of control rat JG cells to AP+40 mmHg-transmural pressure significantly decreased ARC by 19.2±5.2 from 61.8±4.9 to 43.3±4.1 ng

Table 1. Body Weight, Blood Pressure, Urinary Protein Excretion, and Blood Glucose Levels of Control and Diabetes Rats

Model	Body weight (g)	Blood pressure (mmHg)	Urinary protein (mg/day)	Blood glucose (mg/dl)
7 days after peritoneal injections				
Control (n=6)	149±5	120±2	11.3±3.3	122±7
Diabetes (n=6)	120±12*	116±2	14.9±0.8	362±24*
28 days after peritoneal injections				
Control (n=6)	294±6	119±2	15.5±1.4	122±6
Diabetes (n=6)	211±9*	118±2	34.8±4.0*	370±16*

Data are the means±SEM. * $p<0.05$ *vs.* control.

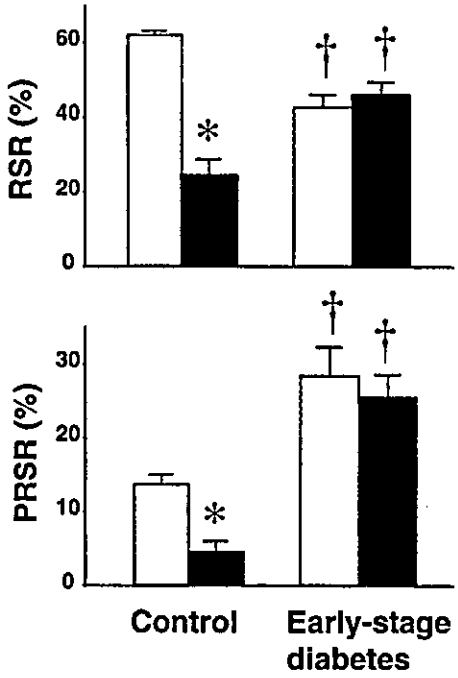

Fig. 1. *Effect of 12-h exposure to atmospheric pressure (open squares) and atmospheric pressure+40 mmHg (closed squares) on renin secretion rate (RSR) and prorenin secretion rate (PRSR) in JG cells from control rats* (n=6) *and rats with early-stage diabetes (DM) intraperitoneally injected with streptozotocin 7 days previously* (n=6). *Data are shown as the means±SEM.* * p<*0.05 for atmospheric pressure+40 mmHg* vs. *atmospheric pressure.* † p<*0.05 for DM* vs. *the controls.*

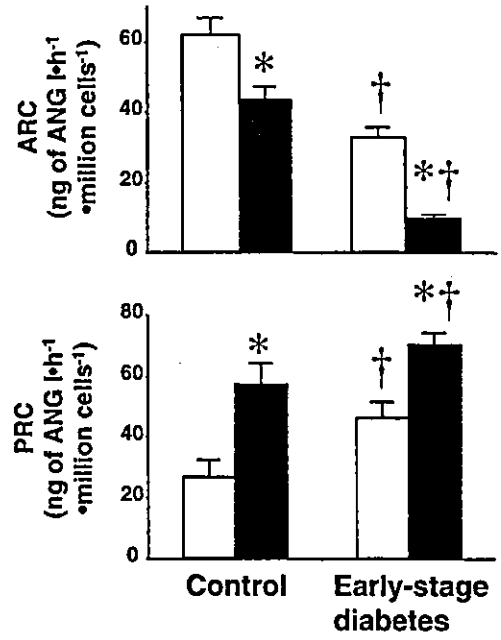

Fig. 2. *Effect of 12-h exposure to atmospheric pressure (open squares) and atmospheric pressure+40 mmHg (closed squares) on active renin content (ARC) and prorenin content (PRC) in JG cells from control rats* (n=6) *and rats with early-stage diabetes (DM) intraperitoneally injected with streptozotocin 7 days previously* (n=6). *Data are shown as means± SEM.* * p< *0.05 for atmospheric pressure+40 mmHg* vs. *atmospheric pressure.* † p<*0.05 for DM* vs. *the controls.*

of Ang I·h^{-1}·million cells^{-1} and significantly increased PRC by 30.7±6.3 from 26.7±5.9 to 57.3±7.0 ng of Ang I·h^{-1}·million cells^{-1}. In JG cells from rats with early-stage streptozotocin-induced diabetes, ARC under AP averaged 32.7±3.1 ng of Ang I·h^{-1}·million cells^{-1} and was significantly less than the ARC in the control rat JG cells. Exposure to AP+40-mmHg transmural pressure significantly decreased ARC by 23.8±3.1 to 9.6±1.4 ng of Ang I·h^{-1}·million cells^{-1}. The decreases in ARC were similar to those observed in control cells. In early-stage diabetes JG cells, PRC under AP averaged 46.4±5.5 ng of Ang I·h^{-1}·million cells^{-1} and was significantly greater than the PRC in the control rat JG cells. Exposure to AP+40-mmHg transmural pressure significantly increased PRC by 23.7±3.5 to 70.1±4.2 ng of Ang I·h^{-1}·million cells^{-1}. The increases in PRC were similar to those observed in control cells. TRC under AP was similar in control cells and early-stage diabetes cells, and exposure to 40-mmHg transmural pressure did not change TRC in control cells or early-stage diabetes cells.

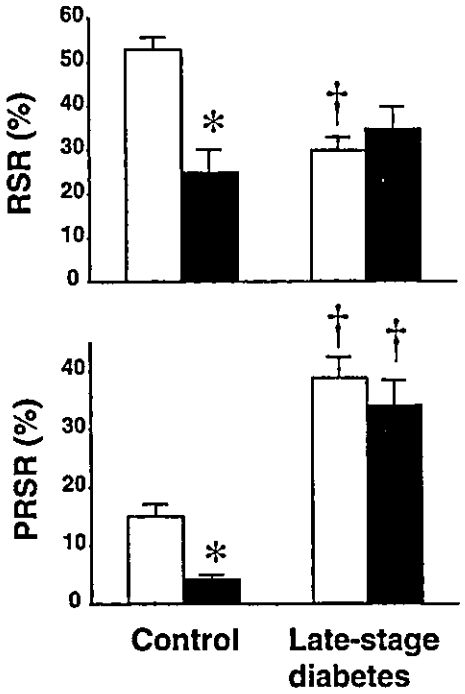

Fig. 3. *Effect of 12-h exposure to atmospheric pressure (open squares) and atmospheric pressure+40 mmHg (closed squares) on renin secretion rate (RSR) and prorenin secretion rate (PRSR) in JG cells from control rats* (n=6) *and rats with late-stage diabetes (DM) intraperitoneally injected with streptozotocin 28 days previously* (n=6). *Data are shown as the means±SEM.* * $p<0.05$ *for atmospheric pressure+40 mmHg* vs. *atmospheric pressure.* † $p<0.05$ *for DM* vs. *the controls.*

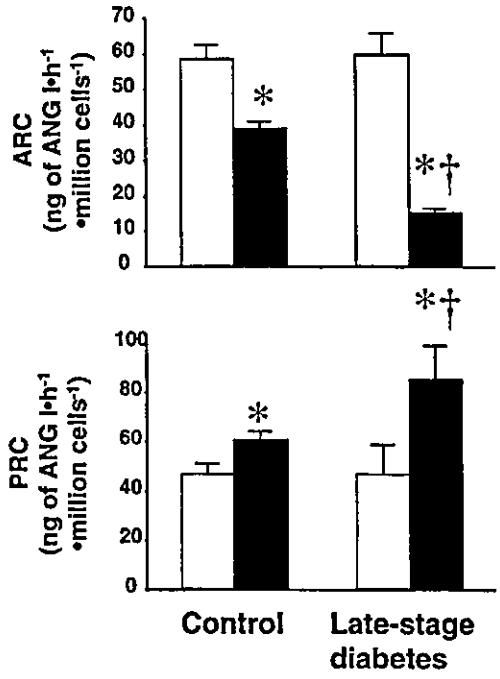

Fig. 4. *Effect of 12-h exposure to atmospheric pressure (open squares) and atmospheric pressure+40 mmHg (closed squares) on active renin content (ARC) and prorenin content (PRC) in JG cells from control rats* (n=6) *and rats with late-stage diabetes (DM) intraperitoneally injected with streptozotocin 28 days previously* (n=6). *Data are shown as means±SEM.* * $p<0.05$ *for atmospheric pressure+40 mmHg* vs. *atmospheric pressure.* † $p<0.05$ *for DM* vs. *the controls.*

Trypan blue exclusion staining of the cells from early-stage diabetes rats yielded similar cell viability values after 12-h loads of AP and AP+40 mmHg.

Transmural Pressure Controls of Prorenin in Late-Stage Diabetes

As shown in Table 1, late-stage diabetes rats have lower body weights, higher levels of blood glucose and urinary protein excretion, and similar levels of systolic blood pressure, compared to control rats. Figure 3 shows the effects of 12-h exposure to transmural pressure on RSR and PRSR in JG cells harvested from rats intraperitoneally injected with control buffer or streptozotocin 28 days previously. Exposure of control rat JG cells to AP+40-mmHg transmural pressure significantly decreased RSR from 52.8±2.9% to 24.9±5.4% and PRSR from 14.9±2.2% to 4.1±1.0%. In the JG cells from the rats with late-stage streptozotocin-induced diabetes, RSR under AP (29.9±3.1%) was significantly lower than in the control rat JG cells. PRSR under AP (38.7±3.7%) was significantly greater than in the control rat JG cells. Neither RSR nor PRSR changed after exposure to AP+ 40-mmHg transmural pressure (34.7± 5.2% and 34.0±4.4%, respectively). Thus, the pressure-induced decreases in RSR and PRSR were also inhibited in late-stage diabetes.

Figure 4 shows a significant decrease in ARC by 19.5± 4.2 from 58.5±4.2 to 38.9±2.2 ng of Ang I·h^{-1}·million $cells^{-1}$ and a significant increase in PRC by 14.0±2.6 from 46.7±4.4 to 60.7±3.5 ng of I·h^{-1}·million $cells^{-1}$, after exposure of control rat JG cells to AP+40-mmHg transmural pressure. In JG cells from rats with late-stage streptozotocin-induced diabetes, ARC under AP (59.7±6.2 ng of Ang I·h^{-1}·million $cells^{-1}$) was similar to the ARC in the control rat JG cells. Exposure to AP+40-mmHg transmural pressure significantly decreased ARC by 44.5±5.1 to 15.1±1.6 ng of Ang I·h^{-1}·million $cells^{-1}$. The decreases in ARC in the cells from the rats with late-stage diabetes were significantly greater than those in the control rat cells. In late-stage diabetes JG cells, PRC under AP (46.7±12.2 ng of Ang I·h^{-1}·million $cells^{-1}$) was similar to the PRC in the control rat JG

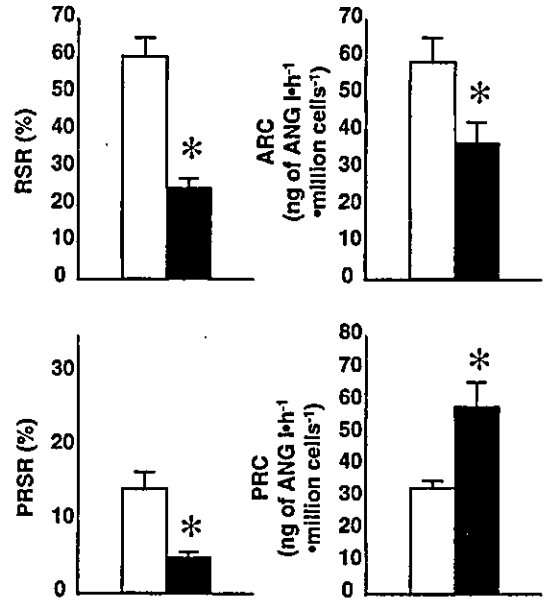

Fig. 5. *Effect of 12-h exposure to atmospheric pressure (open squares) and atmospheric pressure+40 mmHg (closed squares) on renin secretion rate (RSR), prorenin secretion rate (PRSR), active renin content (ARC), and prorenin content (PRC) in JG cells from the rats that were intraperitoneally injected with streptozotocin 28 days previously and continuously received insulin* via *osmotic minipumps during the 4-week period (n=4). Data are shown as the means±SEM. * p<0.05 for atmospheric pressure+40 mmHg* vs. *atmospheric pressure.*

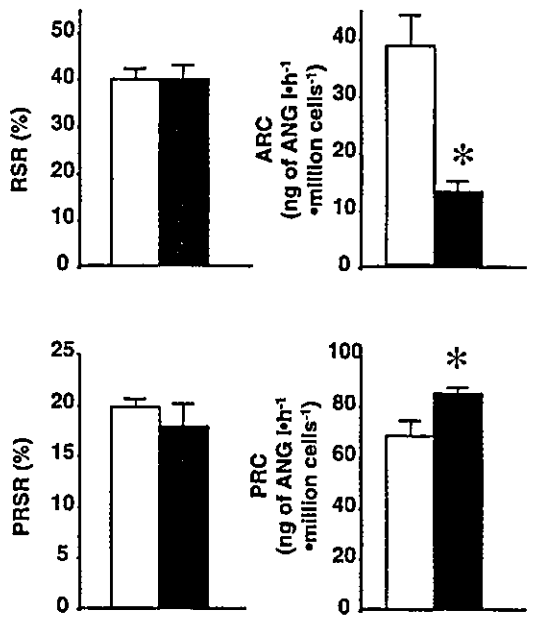

Fig. 6. *Effect of 200 μmol/l NCDC on pressure (atmospheric pressure, open squares; atmospheric pressure+40 mmHg, closed squares) control of renin secretion rate (RSR), prorenin secretion rate (PRSR), active renin content (ARC), and prorenin content (PRC) in the late-stage JG cells of diabetic rats (n=5). * p<0.05 for atmospheric pressure+40 mmHg* vs. *atmospheric pressure.*

cells. Exposure to AP+40-mmHg transmural pressure significantly increased PRC by 34.1±4.6 to 80.7±18.5 ng of Ang I·h^{-1}·million cells^{-1}. The increases in PRC in the cells from the rats with late-stage diabetes were significantly greater than those in the control rat cells. Thus, the pressure-induced decrease in ARC and increase in PRC were enhanced in late-stage diabetes. TRC under AP in the control cells and cells from the rats with late-stage diabetes were similar, and addition of 40 mmHg-transmural pressure did not change TRC in the control cells or cells from the rats with late-stage diabetes. Trypan blue exclusion staining of the cells from the rats with late-stage diabetes showed similar cell viability values after 12-h loads of AP and AP+40 mmHg.

Transmural Pressure Controls of Prorenin in Insulin-Treated Diabetes

Blood glucose levels of the late-stage diabetes rats, which had received insulin *via* minipumps, averaged 124±5 mg/dl (range, 85–171 mg/dl) during the 4-week period and were similar to the blood glucose levels of control rats, which averaged 108±7 mg/dl (range, 89–133 mg/dl). Body weight, systolic blood pressure, and urinary protein excretion of insulin-treated diabetes rats averaged 280±4 g, 115±3 mmHg, and 14.4±1.4 mg/day, respectively. Figure 5 shows the effects of 12-h exposure to transmural pressure on RSR, PRSR, ARC, and PRC in JG cells from the insulin-treated late-stage diabetes rats. In the JG cells, addition of 40 mmHg-transmural pressure significantly decreased RSR, PRSR, and ARC and increased PRC. RSR under AP and AP+40-mmHg averaged 59.8±5.2% and 24.5±2.8%, respectively; PRSR under AP and AP+40-mmHg averaged 14.3±2.2% and 4.8±0.9%, respectively; ARC under AP and AP+40-mmHg averaged 58.5±6.7 and 36.8±5.7 ng of Ang I·h^{-1}·million cells^{-1}, respectively; and PRC under AP and AP+40-mmHg averaged 32.8±2.6 and 58.0±7.9 ng of Ang I·h^{-1}·million cells^{-1}, respectively. However, addition of 40 mmHg-transmural pressure did not change TRC in the JG cells from the insulin-treated late-stage diabetes rats. In the cells from the insulin-treated late-stage diabetes rats, trypan blue exclusion staining showed similar cell viability after 12-h loads of AP and AP+40 mmHg.

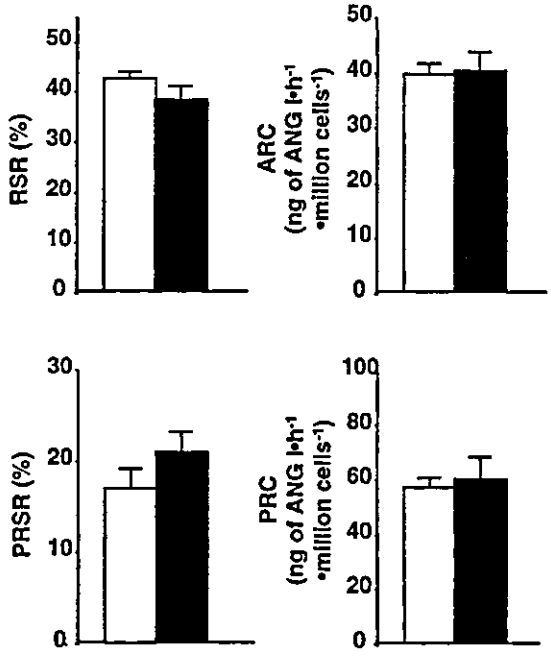

Fig. 7. *Effect of 100 μmol/l AEBSF on pressure (atmospheric pressure, open squares; atmospheric pressure+40 mmHg, closed squares) control of renin secretion rate (RSR), prorenin secretion rate (PRSR), active renin content (ARC), and prorenin content (PRC) in the late-stage JG cells of diabetic rats* (n=5).

Effect of NCDC on Transmural Pressure Controls of Prorenin in Diabetes

Figure 6 shows the effects of 12-h exposure to transmural pressure on RSR, PRSR, ARC, and PRC in late-stage diabetes JG cells incubated in buffer containing 200 μmol/l NCDC. In the JG cells treated with NCDC, RSR under AP and AP+40-mmHg averaged 40.2±2.4% and 40.2±3.2%, respectively; and PRSR under AP and AP+40-mmHg averaged 19.8±0.8% and 17.9±2.3%, respectively. Thus, in the presence of NCDC, transmural pressure did not influence RSR or PRSR of late-stage diabetes JG cells. In the JG cells treated with NCDC, addition of 40 mmHg-transmural pressure significantly decreased ARC from 38.8±5.5 to 13.4±2.0 ng of Ang I•h^{-1}•million cells^{-1} and significantly increased PRC from 68.3±6.4 to 85.0±2.8 ng of Ang I•h^{-1}•million cells^{-1}. Addition of 40 mmHg-transmural pressure did not change TRC in the cells treated with NCDC. In the late-stage diabetes cells treated with 200 μmol/l NCDC, trypan blue exclusion staining showed similar cell viability after 12-h loads of AP and AP+40 mmHg.

Effect of AEBSF on Transmural Pressure Controls of Prorenin in Diabetes

Figure 7 shows the effects of 12-h exposure to transmural pressure on RSR, PRSR, ARC, and PRC in late-stage diabetes JG cells incubated in buffer containing 100 μmol/l AEBSF. In the JG cells treated with AEBSF, RSR under AP and AP+40-mmHg averaged 42.7±1.4% and 38.5±2.8%, respectively, and PRSR under AP and AP+40-mmHg averaged 16.9±2.3% and 21.0±2.3%, respectively. Thus, in the presence of AEBSF, transmural pressure did not influence RSR or PRSR of late-stage diabetes JG cells. However, treatment with AEBSF inhibited the transmural pressure-induced changes in ARC and PRC. In the JG cells treated with AEBSF, ARC under AP and AP+40-mmHg averaged 39.7±2.1 and 40.4±3.4 ng of Ang I•h^{-1}•million cells^{-1}, respectively, and PRC under AP and AP+40-mmHg averaged 57.1±4.0 and 60.2±8.5 ng of Ang I•h^{-1}•million cells^{-1}, respectively. Addition of 40 mmHg-transmural pressure did not change TRC in the cells treated with AEBSF. In the late-stage diabetes cells treated with 100 μmol/l AEBSF, trypan blue exclusion staining showed similar cell viability after 12-h loads of AP and AP+40 mmHg.

Discussion

Chronic transmural pressure loading decreased RSR, PRSR, and ARC and increased PRC in control JG cells without changing TRC. Based on the assumption that there is no intracellular degradation or inactivation of active renin after it is formed from the conversion of prorenin, the results suggest that transmural pressure inhibits exocytosis of renin and prorenin from JG cells and suppresses conversion of prorenin to active renin, consistent with previous studies (*12, 15*). However, exposure of JG cells from rats with early- and late-stage diabetes to a 12-h transmural pressure load decreased ARC and increased PRC without changing RSR, PRSR, or TRC. The magnitude of the PRC elevation was similar in the control and early-stage diabetes JG cells, but a greater increase in PRC was observed in the late-stage diabetes JG cells compared to the control cells and early-stage diabetes JG cells. These results suggest that the development of diabetes mellitus abolishes the transmural pressure effects on prorenin secretion by JG cells and enhances the pressure-mediated inhibition of prorenin processing in JG cells. The impaired pressure control of prorenin secretion was already observed in the early stage of diabetes mellitus and was maintained in the late stage. Thus, transmural pressure is no longer a barrier to prorenin exocytosis from JG cells in diabetes. However, the pressure-induced inhibition of prorenin processing was enhanced in the late-stage diabetes. In the early stage, an evaluation for transmural pressure control of prorenin processing was difficult because ARC under AP was reduced and PRC under AP was elevated in the early-stage diabetes compared to the early-stage controls. Thus,

the pressure-induced inhibition of prorenin processing was unchanged or might be somewhat enhanced in the early-stage diabetes and was certainly enhanced in the late-stage diabetes. Progression of diabetes mellitus causes further accumulation of intracellular prorenin through inhibition of prorenin processing by transmural pressure, and the elevated intrarenal prorenin levels may lead to the increased plasma prorenin levels. These results could explain previous clinical reports demonstrating low renin and high prorenin levels in the blood of diabetics (*1*, *3–7*).

Intracellular calcium plays an important role in the secretion of renin and prorenin from JG cells and is influenced by the calcium receptor system and calcium channels (*16*). Our previous studies demonstrated that PLC-dependent calcium channels contribute to the transmural pressure control of renin secretion by JG cells (*12*, *15*). In afferent arterioles, which transform metaplastically into JG cells (*17*, *18*), streptozotocin-induced diabetes caused functional impairment of voltage-dependent calcium channels (*19*), which are involved in pressure-mediated afferent arteriolar constriction (*20*). In addition, PLC-dependent elevation of intracellular calcium by vasoconstrictors was blunted in mesangial cells exposed to a medium including high glucose levels (*21*). In the present study, the transmural pressure control of prorenin secretion by diabetic JG cells was impaired, and the PLC inhibitor NCDC did not influence the impaired pressure control of prorenin secretion. Since the impaired pressure control of prorenin secretion was already observed in the early-stage diabetes and maintained in the late-stage diabetes, hyperglycemia itself may impair PLC-dependent calcium signals and thereby inhibit the transmural pressure control of secretory exocytosis in JG cells. A previous study reported that high extracellular glucose levels impair intracellular calcium signals through the increased basal intracellular calcium levels due to the pre-activation of stretch receptors by cell shrinkage as a result of the high glucose level (*22*). High extracellular glucose levels are also reported to alter the sensitivity of P2 purinergic receptors (*23*), which are involved in the pressure-mediated constriction of afferent arterioles (*24*), and which mobilize the PLC-dependent intracellular calcium signals (*25*) and inhibit renin secretion (*26*).

The pressure-induced intracellular prorenin accumulation was similar in the control rat JG cells and the JG cells from the rats with early-stage diabetes, but was significantly enhanced in the JG cells from the rats with late-stage diabetes. These results suggest that the enhancement in JG cells may be due to secondary changes during chronic exposure to high extracellular glucose levels. Recent studies have demonstrated that diabetic hyperglycemia causes overproduction of mitochondrial reactive oxygen species (ROS) in vascular endothelial cells (*27*) and that the increased ROS contributes to the progression of arteriosclerosis in diabetes (*28*). Since the PLD-dependent pathways are involved in the ROS production of vascular smooth muscle cells (*29*), chronic exposure to diabetic hyperglycemia may result in the altered activities of PLD-dependent pathways in JG cells. In the present study, the PLD inhibitor AEBSF abolished the pressure-induced intracellular prorenin accumulation observed in the diabetes rat JG cells. Because PLD also contributes to the transmural pressure control of prorenin processing in the JG cells from control rats (*15*), the PLD-dependent pathways play an important role in the pressure control of prorenin processing in either control rat JG cells or diabetes rat JG cells. Further studies are needed to elucidate differences in the PLD-dependent pathways between control rat JG cells and diabetes rat JG cells. In addition, ROS can induce conversion of active renin to inactive renin in JG cells by stimulating the formation of high-molecular-weight renin, that is, a complex between renin and renin-binding protein (*16*). Transmural pressure also stimulates the generation of ROS in arteriolar vascular smooth muscle cells (*30*), and thus transmural pressure and diabetic hyperglycemia may both increase the inactive renin content of JG cells by elevating ROS activity.

In either early-stage or late-stage streptozotocin-induced diabetes, TRC under AP was similar to that in the respective controls, although our preliminary study showed that 12-h exposure of JG cells to 0.1 μg/ml streptozotocin significantly decreases TRC in JG cells (50.2 ± 7.0 and 98.2 ± 2.1 ng of Ang $I \cdot h^{-1} \cdot$million cells^{-1} for the presence and absence of streptozotocin, $n=4$). Therefore, the present observation is not related to acute toxic effects of streptozotocin on JG cells. In addition, normalization of blood glucose levels with the insulin treatment improved the impaired transmural pressure control of prorenin in the late-stage diabetic JG cells. It is therefore unlikely that non-glycemic effects of streptozotocin influence the transmural pressure control of prorenin.

In control rat JG cells, PRC of 28-day rats, averaging 46.7 ng of Ang $I \cdot h^{-1} \cdot$million cells^{-1}, was significantly greater than PRC of 7-day rats, averaging 26.7 ng of Ang $I \cdot h^{-1} \cdot$ million cells^{-1}. These results suggest that aging may cause a renal accumulation of prorenin. Previous studies have demonstrated that subjects over 60 years have a lower plasma concentration of active renin than subjects under 60 years, although total renin concentration was similar in both groups (*31*). Therefore, aging may also suppress activation of prorenin to active renin in the plasma and JG cells.

In conclusion, a 12-h transmural pressure load was found to inhibit processing of prorenin to renin without suppressing prorenin secretion in the JG cells from early-stage diabetes rats, although similar pressure loading suppressed prorenin processing to a similar extent and inhibited prorenin secretion in control JG cells. In the JG cells from the late-stage diabetes rats, a 12-h transmural pressure load also inhibited prorenin processing without suppressing prorenin secretion; however, the transmural pressure-induced inhibition of prorenin processing was significantly greater than that in the control JG cells. These results suggest that both rising pressure and progression of diabetes mellitus cause intrarenal accumulation of prorenin, corresponding to increased plasma prorenin levels in diabetes. In addition, exposure of diabetic

JG cells to the PLD inhibitor AEBSF, but not the PLC inhibitor NCDC, abolished the transmural pressure-induced inhibition of prorenin processing. PLD-dependent pathways play an important role in the prorenin regulation in diabetic JG cells *via* pressure loading.

References

1. Leutscher JA, Kraemer FB, Wilson DM, Schwartz HC, Bryer-Ash M: Increased plasma inactive renin in diabetes mellitus. *N Engl J Med* 1985; **312**: 1412–1417.
2. Taniguchi M, Kim S, Zhan Y, Iwao H: Role of intrarenal angiotensin-converting enzyme in nephropathy of type II diabetic rats. *Hypertens Res* 2002; **25**: 279–285.
3. Daneman D, Crompton CH, Balfe JW, *et al*: Plasma prorenin as an early marker of nephropathy in diabetic (IDDM) adolescents. *Kidney Int* 1994; **46**: 1154–1159.
4. Allen TJ, Cooper ME, Gilbert RE, Winikoff J, Skinner SL, Jerums G: Serum total renin is increased before microalbuminuria in diabetes. *Kidney Int* 1996; **50**: 902–907.
5. Deinum J, Rønn B, Mathiesen E, Derkx FHM, Hop WCJ, Schalekamp MADH: Increase in serum prorenin precedes onset of microalbuminuria in patients with insulin-dependent diabetes mellitus. *Diabetologia* 1999; **42**: 1006–1010.
6. Franken AAM, Derkx FHM, Man-in't-Veld AJ, *et al*: High plasma prorenin in diabetes mellitus and its correlation with some complications. *J Clin Endocrinol Metab* 1990; **71**: 1008–1015.
7. Davies L, Fulcher GR, Atkins A, *et al*: The relationship of prorenin values to microvascular complications in patients with insulin-dependent diabetes mellitus. *J Diabet Complications* 1999; **13**: 45–51.
8. UK Prospective Diabetes Study Group: Tight blood pressure control and risk of macrovascular and microvascular complications in type 2 diabetes: UKPDS 38. *BMJ* 1998; **317**: 703–713.
9. UK Prospective Diabetes Study Group: Efficacy of atenolol and captopril in reducing risk of macrovascular and microvascular complications in type 2 diabetes: UKPDS 39. *BMJ* 1998; **317**: 713–720.
10. Adler A, Stratton IM, Neil HAW, *et al*: Association of systolic blood pressure with macrovascular and microvascular complications of type 2 diabetes (UKPDS 36): prospective observational study. *BMJ* 2000; **321**: 412–419.
11. Takiuchi S, Rakugi H, Masuyama T, *et al*: Hypertension attenuates the efficacy of hypoglycemic therapy for preserving coronary flow reserve in patients with type 2 diabetes. *Hypertens Res* 2002; **25**: 893–900.
12. Ichihara A, Suzuki H, Miyashita Y, Naitoh M, Hayashi M, Saruta T: Transmural pressure inhibits prorenin processing in juxtaglomerular cell. *Am J Physiol* 1999; **277**: R220–R228.
13. Ichihara A, Suzuki H, Murakami M, Naitoh M, Matsumoto A, Saruta T: Interactions between angiotensin II and norepinephrine on renin release by juxtaglomerular cells. *Eur J Endocrinol* 1995; **133**: 569–577.
14. Ichihara A, Kobori H, Miyashita Y, Hayashi M, Saruta T: Differential effects of thyroid hormone on renin secretion, content, and mRNA in juxtaglomerular cells. *Am J Physiol* 1998; **274**: E224–E237.
15. Hirota N, Ichihara A, Koura Y, Hayashi M, Saruta T: Phospholipase D contributes to transmural pressure control of prorenin processing in juxtaglomerular cell. *Hypertension* 2002; **39**: 363–367.
16. King JA, Lush DJ, Fray JCS: Regulation of renin processing and secretion: chemiosmotic control and novel secretory pathway. *Am J Physiol* 1993; **265**: C305–C320.
17. Barajas L: Anatomy of the juxtaglomerular apparatus. *Am J Physiol* 1979; **237**: F333–F343.
18. Taugner R, Bührle CP, Hackenthal E, Mannek E, Nobiling R: Morphology of the juxtaglomerular apparatus and secretory mechanisms. *Contrib Nephrol* 1984; **43**: 76–101.
19. Carmines PK, Ohishi K, Ikenaga H: Functional impairment of renal afferent arteriolar voltage-gated calcium channels in rats with diabetes mellitus. *J Clin Invest* 1996; **98**: 2564–2571.
20. Takenaka T, Suzuki H, Okada H, Hayashi K, Kanno Y, Saruta T: Mechanosensitive cation channel mediate afferent arteriolar myogenic constriction in the isolated rat kidney. *J Physiol (Lond)* 1998; **511**: 245–253.
21. Mene P, Pugliese G, Pricci F, Di-Mario U, Cinotti GA, Pugliese F: High glucose inhibits cytosolic calcium signaling in cultured rat mesangial cells. *Kidney Int* 1993; **43**: 585–591.
22. Symonian M, Smogorzewski M, Marcinkowski W, Krol E, Massry SG: Mechanisms through which high glucose concentration raises $[Ca^{2+}]_i$ renal proximal tubular cells. *Kidney Int* 1998; **54**: 1206–1213.
23. Solini A, Chiozzi P, Falzoni S, Morelli A, Fellin R, Di-Virgilio F: High glucose modulates $P2X_7$ receptor-mediated function in human primary fibroblasts. *Diabetologia* 2000; **43**: 1248–1256.
24. Inscho EW, Cook AK, Navar LG: Pressure-mediated vasoconstriction of juxtamedullary afferent arterioles involves P2-purinoceptor activation. *Am J Physiol* 1996; **271**: F1077–F1085.
25. Dubyak GR, El-Moatassim C: Signal transduction *via* P2-purinergic receptors for extracellular ATP and other nucleotides. *Am J Physiol* 1993; **265**: C577–C606.
26. Bader M, Ganten D: Regulation of renin: new evidence from cultured cells and genetically modified mice. *J Mol Med* 2000; **78**: 130–139.
27. Nishikawa T, Edelstein D, Du XL, *et al*: Normalizing mitochondrial superoxide production blocks three pathways of hyperglycaemic damage. *Nature* 2000; **404**: 787–790.
28. Shinomiya K, Fukunaga M, Kiyomoto H, *et al*: A role of oxidative stress-generated eicosanoid in the progression of arteriosclerosis in type 2 diabetes mellitus model. *Hypertens Res* 2002; **25**: 91–98.
29. Touyz RM, Schiffrin EL: Ang II-stimulated superoxide production is mediated *via* phospholipase D in human vascular smooth muscle cells. *Hypertension* 1999; **34**: 976–982.
30. Nowicki PT, Flavahan S, Hassanain H, *et al*: Redox signaling of the arteriolar myogenic response. *Circ Res* 2001; **89**: 114–116.
31. Higaki J, Morishita R, Ogihara T, Nishiura M: Effects of aging on human plasma renin: simultaneous multiple assays of enzyme activity and immunoactivity of plasma renin. *Acta Endocrinol* 1989; **120**: 81–86.

Original Article

Angiotensin II Type 2 Receptor Inhibits Prorenin Processing in Juxtaglomerular Cells

Atsuhiro ICHIHARA, Matsuhiko HAYASHI, Nobuhisa HIROTA, Hirokazu OKADA*, Yukako KOURA, Yuko TADA, Yuki KANESHIRO, Hirohiko TSUGANEZAWA, and Takao SARUTA

Long-term treatment with an angiotensin II type 1 receptor blocker (ARB) has been shown to decrease the plasma renin activity (PRA) of hypertensive patients, whereas PRA remains elevated during angiotensin-converting enzyme inhibitor (ACEI) treatment. In the present study, we used rat juxtaglomerular (JG) cells to elucidate the mechanism(s) involved in the differential regulation of PRA between ARB and ACEI treatment. Addition of 100 nmol/l angiotensinogen (Aogen) to JG cells (n=6 primary cultures) significantly increased the medium angiotensin (Ang) II levels from 14±2 to 440±9 pg/ml and suppressed the renin secretion rate (RSR) from 39.6±5.4% to 6.3±1.8% without affecting active renin content (ARC) or total renin content (TRC). In the Aogen-treated cells, the ACEI, delapril hydrochloride (CV3317, 10 μmol/l), significantly decreased the medium Ang II levels to 58±14 pg/ml and increased RSR to 39.8±4.1% without affecting ARC or TRC. The ARB, an active metabolite of candesartan cilexetil (CV11974, 10 μmol/l), however, significantly increased the medium Ang II levels and RSR to 486±15 pg/ml and 40.9±9.8%, respectively, and decreased ARC from 63.2±6.8 to 21.6±3.6 ng of Ang I·h^{-1}·million cells^{-1} without affecting TRC. The decreases in ARC of the Aogen+CV11974-treated cells (n=6 primary cultures) were inhibited by an Ang II type 2 receptor blocker, PD123319 (10 μmol/l). JG cells (n=6 primary cultures) were also treated with an Ang II type 2 receptor agonist, CGP42212A (0.1 μmol/l). CGP42212A significantly increased RSR from 38.2±1.6% to 49.7±4.7% and decreased ARC from 60.8±3.0 to 25.3±2.8 ng of Ang I·h^{-1}·million cells^{-1} without affecting TRC. Addition of CV11974 did not alter the RSR, ARC, or TRC of the CGP42212A-treated cells; however, PD123319 abolished the effects of CGP42212A. These results indicate that, distinct from ACEIs, ARBs inhibit prorenin processing of JG cells through Ang II type 2 receptors. Long-term treatment with an ARB may decrease PRA in part by diminishing the storage of active renin in JG cells. (*Hypertens Res* 2003; 26: 915–921)

Key Words: **renin-angiotensin system, angiotensinogen, angiotensin-converting enzyme inhibitors, angiotensin receptor blockers, prorenin**

Introduction

Angiotensin II type 1 receptor blockers (ARBs) completely inhibit all physiological effects of angiotensin type 1 (AT1) receptors, including the negative feedback loop of renin secretion. During ARB treatment, therefore, renin secretion from juxtaglomerular (JG) cells should be increased, and the increased plasma renin levels should lead to elevation of plasma angiotensin (Ang) II levels, resulting in predominant

From the Department of Internal Medicine, Keio University School of Medicine, Tokyo, Japan, and *Internal Medicine, Saitama Medical College, Saitama, Japan.

This work was supported in part by Grants-in-Aid for Scientific Research from the Ministry of Education, Culture, Sports, Science, and Technology of Japan (14571073) and from the Japan Arteriosclerosis Prevention Fund.

Address for Reprints: Atsuhiro Ichihara, M.D., Instructor of Internal Medicine, Keio University School of Medicine, 35 Shinanomachi, Shinjuku-ku, Tokyo 160-8582, Japan. E-mail: atzichi@sc.itc.keio.ac.jp

Received June 11, 2003; Accepted in revised form July 25, 2003.

stimulation of angiotensin type 2 (AT2) receptors. Because AT2 receptor is reported to antagonize the pressor effects and cell-proliferative actions of AT1 receptor and increase plasma bradykinin levels (*1*, *2*), ARBs would seem to have advantages over angiotensin-converting enzyme inhibitors (ACEIs) in terms of conferring protection from hypertensive organ damage. In addition, ACEIs may have some disadvantages, because a chymase can generate Ang II during ACEI treatment. It is therefore reasonable to expect that the overall clinical benefits of ARBs would be superior to those of ACEIs. However, clinical studies have demonstrated that ARBs and ACEIs are equivalent in protecting systemic organs, including the heart and kidneys, from hypertensive damage (*3–8*).

In a recent clinical report, long-term treatment with an ARB restored or decreased plasma renin activity of hypertensive patients to the baseline level or lower, although plasma renin activity remained elevated during the ACEI treatment (*9*), and in another study, the increase in plasma renin activity during long-term treatment with an ARB was smaller than that observed during long-term treatment with an ACEI (*10*). These novel findings suggest that ARB treatment may have some negative influences on plasma renin control, and thus the stimulation of AT2 receptors during ARB treatment may be less than expected.

The present study was designed to delineate the differential effects of ARB and ACEI on renin synthesis and secretion at the level of JG cells. For this purpose, rat JG cells were incubated with the culture medium containing a recombinant angiotensinogen, and the synthesis and secretion of active renin were evaluated in the presence or absence of an ARB and ACEI. In addition, the agonist and antagonist for AT2 receptors were added to JG cells to determine the contribution of AT2 receptors to the ARB effects on renin regulation.

Methods

Primary Culture of Rat JG Cells

In accordance with the guidelines and practices established by the Keio University Animal Care and Use Committee, JG cells were isolated from kidneys of male Sprague-Dawley rats (100–150 g) as previously described (*11–14*). JG cells were suspended at 10^6 cells/ml in culture medium consisting of RPMI 1640 with 25 mmol/l *N*-2-hydroxyethylpiperazine-*N'*-2-ethane sulfonic acid, 0.3 g/l L-glutamine, 100 μg/ml streptomycin, 100 U/ml penicillin, 0.66 U/l insulin, and 10% fetal bovine serum. Cell number was determined using a Coulter counter. The suspended cells were distributed in 1 ml aliquots into individual wells of 8-well chamber slides containing 1 ml of culture medium and incubated at 37°C. JG cells had a 48-h rest period before the beginning of the experiments. Immunofluorescence staining for renin confirmed that 87±4% of the cells ($n=5$ primary cultures) were positive for renin at 60 h after isolation (*11–14*).

Immunocytochemical Detection of Renin and AT1/AT2 Receptors by Confocal Laser Microscopy

Primary JG cells grown on LabTek chamber slides (154917; Nalgene Nunc, Tokyo, Jpan) were fixed with 4% paraformaldehyde for 20 min and prehybridized with Protein Block Serum-Free (Dako, Capinteria, USA). Cells were then incubated overnight at room temperature with mouse monoclonal anti-renin antibody against rat renin antibody (Swant, Bellinzona, Switzerland) at a dilution of 1:50, followed by 1 h-incubation with FITC-conjugated goat polyclonal anti-mouse IgG (1:500; American Qualex, San Clemente, USA) at room temperature. Cells were then incubated overnight at room temperature with the rabbit anti-AT1 receptor antibody (Santa Cruz Biotech, Santa Cruz, USA) at a dilution of 1:200, followed by 1 h-incubation with AlexaFluor 647 goat anti-rabbit IgG (1:500; Molecular Probes, Eugene, USA) at room temperature. To detect AT2 receptor, goat polyclonal anti-AT2 receptor antibody (Santa Cruz Biotech) was used at a dilution of 1:200 as a primary antibody, and visualized with FITC-conjugated rabbit polyclonal anti-goat IgG (Sigma, St. Louis, USA) at a dilution of 1:500. The cells were mounted in Vectashield (Vector Laboratories, Burlingame, USA) containing PI (Sigma) for nuclear staining. After isolating the secondary antibody by immunoaffinity chromatography, a sample from which the primary antibodies had been omitted was used as a negative control. For confocal imaging, a Bio-Rad Radiance 2000 laser scanning microscope (Bio-Rad, Tokyo, Japan) was used at constant system setting, and digitally captured images were deconvolved with Laser Sharp2000 (Bio-Rad) imaging software.

Measurement of Renin Secretion Rate, Active Renin Content, and Total Renin Content in JG Cells

The renin secretion rate (RSR), active renin content (ARC), and total (active+inactive) renin content (TRC) were measured in JG cells as described previously (*13*, *14*). In brief, after the culture medium had been removed, the cells were washed twice with pre-warmed phosphate buffered saline (PBS). Each well was filled with 1 ml of Ca^{2+}-containing PBS. Immediately before (0 h) and at 12 h of culture, the cell-conditioned buffer was removed and centrifuged. The supernatants were stored at −20°C until renin activity was assayed for determination of RSR. After rinsing with PBS, the cells were frozen in liquid nitrogen and stored at −80°C. For assay of ARC and TRC, frozen cells were homogenized in 1 ml of buffer (pH 6.0) containing 2.6 mmol/l ethylenediaminetetraacetate, 1.6 mmol/l dimercaprol, 3.4 mmol/l 8-hydroxyquinoline sulfate, 0.2 mmol/l phenylmethylsulfonyl fluoride, and 5 mmol/l ammonium acetate. The homogenates were centrifuged at 12,000×*g* for 30 min, and the supernatant was removed. To measure TRC in JG cells, the sam-

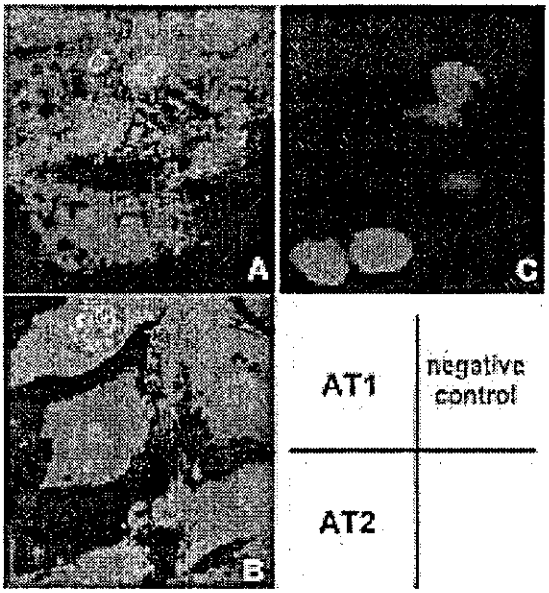

Fig. 1. *Immunocytochemical detection of renin and AT1 receptors by confocal laser microscopy. In the cells containing a nucleus (shown in red) and renin granules (shown in green), AT1 receptors (shown in purple) were present both at the cell surface and in the cytoplasm (A). AT2 receptors (shown in blue) were also observed both at the cell surface and in the cytoplasm (B). The negative control without primary antibodies did not have any non-specific signals (C).*

ples (900 μl) were incubated at 0 °C for 60 min with 100 μl of 4 mg/ml trypsin (Sigma) in 500 mmol/l Tris buffer, pH 7.5, containing 5 mmol/l $CaCl_2$, 0.1% NaCl azide, and 1% bovine serum albumin, as described previously (*14*). Soybean trypsin inhibitor (Sigma; 8 mg/ml final concentration) was added to stop the reaction. Thus, inactive renin in the samples was converted to active renin, and renin activity was then determined.

Renin activity was determined as previously described (*12*). Samples were incubated for 1 h at 37 °C with plasma from bilaterally nephrectomized male Sprague-Dawley rats as the renin substrate, and renin activity was determined by the generation of Ang I from a plasma angiotensinogen substrate. Ang I levels were measured using a radioimmunoassay coated-bead kit from Dinabott Radioisotope Institute. RSR (%) was calculated as the fractional release of overall active renin (*i. e.*, [buffer renin activity at 12 h − buffer renin activity at 0 h]/[active renin content in JG cells at 12 h + buffer renin activity at 12 h − buffer renin activity at 0 h]). JG cell ARC and TRC were expressed as the renin activity of the sample obtained per million cells.

Experimental Protocols

Primary JG cell cultures were divided into four groups, with each group including at least 2 wells, and the mean values per primary culture were determined in each group. In the first series of experiments, we assessed the effects of recombinant sheep angiotensinogen (Aogen, 100 nmol/l) (*15*) on renin synthesis and secretion in JG cells. The cells were conditioned in control buffer or buffer containing CV3317 (delapril hydrochloride, 10 μmol/l) as an ACEI and CV11974 (an active metabolite of candesartan cilexetil, 10 μmol/l) as an ARB. The amounts of Ang II generated from Aogen in the culture media with or without Aogen, Aogen + ACEI, or Aogen + ARB were determined by radioimmunoassay. In the second series of experiments, which examined the involvement of AT1 and AT2 receptors in the effects of Aogen on renin regulation, the cells were conditioned in buffer containing the AT1 receptor blocker, CV11974 (10 μmol/l), the AT2 receptor blocker, PD123319 (10 μmol/l; Sigma), or both. The effects of the AT2 receptor agonist, CGP42212A (0.1 μmol/l, Sigma) on renin regulation were examined in the third series of experiments. The cells were conditioned in control buffer or buffer containing CV11974 (10 μmol/l) and PD123319 (10 μmol/l). Aogen was a gift from Dr. Fumiaki Suzuki (Gifu University, Gifu, Japan). CV3317 and CV11974 were provided by Takeda Chemical Industries (Osaka, Japan).

Statistical Analysis

Data were analyzed by two-way ANOVA followed by multiple comparisons using Scheffé's *F*-test for repeated measures. A value of $p < 0.05$ was considered statistically significant. Data are shown as the means ± SEM.

Results

AT1 and AT2 Receptors of JG Cells

Figure 1 shows the immunocytochemical colocalization of renin and AT receptors. In JG cells containing renin granules, AT1 receptor signals were observed not only on the cell surface but also in the cytoplasm, and these signals were eradicated by preabsorbing the antibodies with the competing peptide (Santa Cruz Biotech) (data not shown). AT2 receptor signals were also observed both on the cell surface and in the cytoplasm, but AT2 receptors were observed separately from renin granules because of their lower expression level. No competing peptide against the AT2 receptor antibody used in the present study is currently available. In the absence of primary antibodies, however, no signals other than those in the nucleus were observed. These results were consistent with previous studies demonstrating an immunohistochemical localization of AT1 receptor (*16–19*) or AT2 receptor (*19*) in the JG apparatus and a biochemical localization of AT2 receptor in afferent arterioles (*20*) which transform metaplastically into JG cells (*21, 22*).

Table 1. Angiotensin II Concentrations in Culture Medium

	Treatments			
	Control	Aogen	Aogen+ACEI	Aogen+ARB
Angiotensin II (pg/ml)	14±2	440±9*	58±14*,†	486±15*,†

Data are the means±SEM. Aogen, angiotensinogen (100 nmol/l); ACEI, CV3317 (10 μmol/l); ARB, CV11974 (10 μmol/l). The experiment was performed with 6 primary cultures. *$p<0.05$ *vs.* control. †$p<0.05$ *vs.* Aogen.

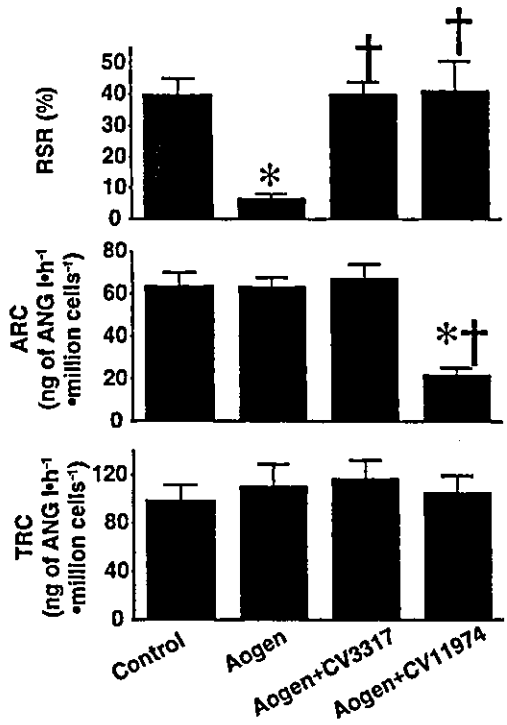

Fig. 2. *Effects of 100 nmol/l recombinant sheep angiotensinogen (Aogen) on renin secretion rate (RSR), active renin content (ARC), and total renin content (TRC) in juxtaglomerular cells incubated with control buffer or buffer containing ACEI (CV3317, 10 μmol/l) and angiotensin II type 1 receptor blocker (ARB; CV11974, 10 μmol/l). The experiment was performed with 6 primary cultures.* *$p<0.05$ vs. *control.* †$p<0.05$ vs. *Aogen alone.*

Effects of Angiotensinogen on JG Cells Treated with ACEI and ARB

Table 1 shows Ang II concentrations in the culture medium of untreated JG cells and the cells treated with Aogen alone, Aogen+CV3317, or Aogen+CV11974. In the Aogen-treated JG cells, the medium Ang II levels significantly increased compared to those in untreated JG cells, and the increases were attenuated by addition of an ACEI, CV3317, and enhanced by addition of an ARB, CV11974.

Figure 2 demonstrates the effects of Aogen on the RSR, ARC, and TRC of the JG cells incubated with control buffer or buffer containing an ACEI, CV3317, and an ARB, CV11974. The RSR, ARC, and TRC of JG cells treated with control buffer averaged 39.6±5.4%, 63.2±6.8 ng of Ang I·h^{-1}·million cells^{-1}, and 98.0±13.5 ng of Ang I·h^{-1}·million cells^{-1}, respectively. Addition of Aogen to the culture medium significantly decreased RSR to 6.3±1.8% but did not alter ARC or TRC. In the presence of CV3317, Aogen did not influence RSR, ARC, or TRC of JG cells. The RSR of JG cells treated with Aogen+ACEI (CV3317) averaged 39.8±4.1% and was similar to that of JG cells treated with control buffer. In the presence of CV11974, however, Aogen significantly reduced ARC to 21.6±3.6 ng of Ang I·h^{-1}·million cells^{-1} without affecting RSR or TRC. The RSR of JG cells treated with Aogen+ARB (CV11974) averaged 40.9±9.8% and was similar to that of JG cells treated with control buffer.

Functions of AT1 and AT2 Receptors in JG Cells

Figure 3 demonstrates the effects of the AT1 receptor blocker CV11974, the AT2 receptor blocker PD123319, or both on RSR, ARC, and TRC in the Aogen-treated JG cells. The RSR, ARC, and TRC of the Aogen-treated JG cells averaged 9.0±1.2%, 58.5±4.5 ng of Ang I·h^{-1}·million cells^{-1}, and 102.5±6.4 ng of Ang I·h^{-1}·million cells^{-1}, respectively. Addition of CV11974 to the culture medium of the Aogen-treated JG cells significantly increased RSR to 50.5±5.5% and significantly decreased ARC to 20.2±2.7 ng of Ang I·h^{-1}·million cells^{-1} without affecting TRC. Addition of PD123319 did not significantly influence the RSR, ARC, or TRC of the Aogen-treated JG cells. In the Aogen-treated JG cells, however, treatment with both CV11974 and PD123319 significantly increased RSR to 39.7±2.1% and did not influence ARC or TRC. The RSR of JG cells treated with Aogen+CV11974+PD123319 was significantly greater than that of the Aogen-treated cells or Aogen+PD123319-treated cells and similar to that of the Aogen+CV11974-treated cells. The ARC of JG cells treated with Aogen+CV11974+PD123319 was significantly greater than that of the Aogen+CV11974-treated cells and similar to that of the Aogen-treated cells or the Aogen+PD123319-treated cells.

Figure 4 shows the effects of the AT2 receptor agonist CGP42212A on RSR, ARC, and TRC of JG cells incubated with control buffer or buffer containing the AT1 receptor blocker CV11974 and the AT2 receptor blocker PD123319.